Atmospheric
Chemistry
and Physics
Discussions

Open Access

# Biomass burning emissions and potential air quality impacts of volatile organic compounds and other trace gases from temperate fuels common in the United States

J. B. Gilman[1,2], B. M. Lerner[1,2], W. C. Kuster[1,2,a], P. D. Goldan[1,2,a], C. Warneke[1,2], P. R. Veres[1,2], J. M. Roberts[2], J. A. de Gouw[1,2], I. R. Burling[3,b], and R. J. Yokelson[3]

[1]CIRES at University of Colorado, Boulder, CO, USA
[2]NOAA Earth System Research Laboratory, Boulder, CO, USA
[3]Department of Chemistry, University of Montana, Missoula, Montana, USA
[a]now retired
[b]now at: Cytec Canada, Niagara Falls, Ontario, Canada

Title Page

Abstract | Introduction

Conclusions | References

Tables | Figures

|◄ | ►|

◄ | ►

Back | Close

Full Screen / Esc

Printer-friendly Version

Interactive Discussion

Full Screen / Esc

## Abstract

A comprehensive suite of instruments was used to quantify the emissions of over 200 organic gases, including methane and volatile organic compounds (VOCs), and 9 inorganic gases from 56 laboratory burns of 18 different biomass fuel types common in the southeastern, southwestern, or northern United States. A gas chromatograph-mass spectrometer (GC-MS) provided extensive chemical detail of discrete air samples collected during a laboratory burn and was complemented by real-time measurements of organic and inorganic species via an open-path Fourier transform infrared spectrometer (OP-FTIR) and 3 different chemical ionization-mass spectrometers. These measurements were conducted in February 2009 at the U.S. Department of Agriculture's Fire Sciences Laboratory in Missoula, Montana. The relative magnitude and composition of the gases emitted varied by individual fuel type and, more broadly, by the 3 geographic fuel regions being simulated. Emission ratios relative to carbon monoxide (CO) were used to characterize the composition of gases emitted by mass; reactivity with the hydroxyl radical, OH; and potential secondary organic aerosol (SOA) precursors for the 3 different US fuel regions presented here. VOCs contributed less than $0.78 \pm 0.12$ % of emissions by mole and less than $0.95 \pm 0.07$ % of emissions by mass (on average) due to the predominance of $CO_2$, CO, $CH_4$, and $NO_x$ emissions; however, VOCs contributed 70–90 ($\pm 16$) % to OH reactivity and were the only measured gas-phase source of SOA precursors from combustion of biomass. Over 82 % of the VOC emissions by mole were unsaturated compounds including highly reactive alkenes and aromatics and photolabile oxygenated VOCs (OVOCs) such as formaldehyde. OVOCs contributed 57–68 % of the VOC mass emitted, 42–57 % of VOC-OH reactivity, and aromatic-OVOCs such as benzenediols, phenols, and benzaldehyde were the dominant potential SOA precursors. In addition, ambient air measurements of emissions from the Fourmile Canyon Fire that affected Boulder, Colorado in September 2010 allowed us to investigate biomass burning (BB) emissions in the presence of other VOC

sources (i.e., urban and biogenic emissions) and identify several promising BB markers including benzofuran, 2-furaldehyde, 2-methylfuran, furan, and benzonitrile.

# 1 Introduction

Biomass burning (BB) emissions are composed of a complex mixture of gases and
5  particles that may directly and/or indirectly affect both climate and air quality (Jaffe and Wigder, 2012; Sommers et al., 2014). Emissions include greenhouse gases such as carbon dioxide ($CO_2$), methane ($CH_4$), and nitrous oxide ($N_2O$); carcinogens such as formaldehyde and benzene; and other components harmful to human health including particulate matter, carbon monoxide (CO) and isocyanic acid (HNCO) (Crutzen and
10  Andreae, 1990; Hegg et al., 1990; Andreae and Merlet, 2001; Demirbas and Demirbas, 2009; Estrellan and Iino, 2010; Roberts et al., 2010, 2011; Sommers et al., 2014). The co-emission of nitrogen oxides ($NO_x = NO + NO_2$) and reactive volatile organic compounds (VOCs, also known as non-methane organic compounds) from combustion of biomass may degrade local and regional air quality by the photochemical formation
15  of tropospheric ozone ($O_3$), a hazardous air pollutant, and secondary organic aerosol (SOA) (Alvarado et al., 2015). This work is aimed at characterizing primary biomass burning emissions of organic and inorganic gases in order to identify key species that may contribute to $O_3$ and/or SOA formation.

Tropospheric $O_3$ may be formed in the atmosphere from the interactions of VOCs,
20  $NO_x$, and a radical source such as the hydroxyl radical (OH), which is formed from the photolysis of $O_3$, aldehydes, hydroperoxides, or nitrous acid (HONO). OH is a key oxidant in the troposphere and it plays a pivotal role in determining the atmospheric lifetimes of reactive organic and inorganic gases. Oxidation of VOCs and other gases such as CO and $CH_4$ by OH leads to the formation of alkyl (R•), alkoxy (RO•), and
25  alkylperoxy ($RO_2$•) radicals, where R represents a carbon-containing derivative. These radicals are important, but short-lived, intermediaries that aid in the conversion of NO to $NO_2$. Photolysis of $NO_2$ produced from the reaction of $RO_2$• + NO is the principal

**Biomass burning emissions and potential air quality impacts**

J. B. Gilman et al.

Title Page

| Abstract | Introduction |
| Conclusions | References |
| Tables | Figures |

Back | Close

Full Screen / Esc

Printer-friendly Version

Interactive Discussion

source of tropospheric $O_3$; however, the amount of $O_3$ formed is dependent on the relative abundances of $NO_x$ and VOCs (Carter, 1994). Biomass burning is a large, primary source of VOCs, $NO_x$, and HONO (i.e., $O_3$ precursors); however, these species are emitted at varying relative ratios depending on the fuel type and burn conditions making it difficult to predict $O_3$ formation from the combustion of biomass (Akagi et al., 2011; Jaffe and Wigder, 2012). An additional $O_3$ formation pathway involves the formation of peroxynitrates, such as peroxyacetic nitric anhydride (PAN), via $R(O)O_2\bullet + NO_2$ reaction. This pathway may diminish $O_3$ formation in fresh BB plumes due to the initial sequestration of $NO_2$, but enhance $O_3$ downwind formation via production of $NO_2$ from thermal dissociation of peroxynitrates (Jaffe and Wigder, 2012).

SOA is organic particulate mass that is formed in the atmosphere from the chemical evolution of primary emissions of organic species. Here, chemical evolution refers to a complex series of reactions of a large number of organic species that results in the formation of relatively low volatility and/or high solubility oxidation products that will readily partition to, or remain in, the particle phase (Kroll and Seinfeld, 2008). Oxidation may occur via addition of OH, $O_3$, or the nitrate radical ($NO_3$) to a double bond or result from the reactions of the $RO_2\bullet$ and/or $RO\bullet$ radicals formed from hydrogen abstraction of the parent compound. These pathways may result in oxidation products that contain polar functional groups such as ketones, aldehydes, alcohols, nitrates, and carboxylic acids that can have vapor pressures approximately 10 to 10 000 times lower than their parent compounds (Pankow, 1994) allowing for more efficient partitioning to the particulate phase. Thus, VOCs that are considered to be efficient SOA precursors are relatively reactive organic compounds whose oxidation products are of sufficiently low volatility and/or higher solubility than the parent VOC. SOA formation from BB emissions is highly variable and chemical modeling results suggest that there is a "missing large source of SOA" precursors that cannot be explained by known SOA precursors such as toluene (Alvarado et al., 2015).

Advances in instrumentation and complementary measurement approaches have enabled chemical analyses of a wide range of species emitted during laboratory-based

**Biomass burning emissions and potential air quality impacts**

J. B. Gilman et al.

Title Page

| Abstract | Introduction |
| Conclusions | References |
| Tables | Figures |

|◀ | ▶|
◀ | ▶

Back | Close

Full Screen / Esc

Printer-friendly Version

Interactive Discussion

biomass burning experiments (Yokelson et al., 1996, 2013; McDonald et al., 2000; Schauer et al., 2001; Christian et al., 2003; Veres et al., 2010; Hatch et al., 2015; Stockwell et al., 2015). This information supplements several decades of field measurements of BB emissions reported in the literature (Andreae and Merlet, 2001; Friedli et al., 2001; Akagi et al., 2011; Simpson et al., 2011). Chemically detailed, representative measurements of VOCs and other trace gases from biomass combustion are critical input to photochemical transport models aimed at reproducing observed downwind changes in the concentrations of reactive species including VOCs, $O_3$, peroxynitrates, and organic aerosol (Trentmann et al., 2003, 2005; Mason et al., 2006; Alvarado and Prinn, 2009; Heilman et al., 2014; Urbanski, 2014; Alvarado et al., 2015) and are essential to understanding impacts on chemistry, clouds, climate, and air quality.

For this study, a comprehensive suite of gas-phase measurement techniques was used to quantify the emissions of 200 organic gases, including methane and VOCs, and 9 inorganic gases from laboratory biomass burns of 18 fuel types from 3 geographic regions in the US (hereafter referred to as "fuel regions") in order to examine the potential atmospheric impacts of these gaseous emissions. We focus on the 56 fires sampled by a gas chromatograph-mass spectrometer (GC-MS), which is limited to sampling a relatively short, discrete segment of a laboratory burn. We begin by comparing mixing ratios measured by the GC-MS to those measured by infrared spectroscopy and proton-transfer-reaction mass spectrometry, both of which provide near-continuous sampling of laboratory fires. We then compare discrete ERs and fire-integrated ERs, representing the entirety of emissions from a laboratory burn, in order to quantify any potential bias that resulted from discrete vs. "continuous" sampling techniques.

In order to merge and compare datasets from multiple instruments, we report mean discrete emission ratios (ER) of the measured gases relative to CO for southwestern, southeastern, and northern fuel regions. Previous publications present fire-integrated ERs for the real-time measurement techniques (Veres et al., 2010; Warneke et al., 2011), fuel-based emissions factors (Burling et al., 2010; Yokelson et al., 2013), and comparisons between laboratory and field measurements of BB emissions (Burling

et al., 2010, 2011; Yokelson et al., 2013). Yokelson et al. (2013) focused on retrieving an improved set of emission factors for prescribed fires by coupling lab and field work, but they performed only a cursory analysis of the atmospheric impacts. This paper provides a more detailed examination of the chemical composition of BB emissions from fires simulating each fuel region in order to identify key species that may impact air quality through formation of $O_3$ and/or SOA. We compare the chemical composition of the mass emitted, the reactivities of the measured gases with the hydroxyl radical in order to identify the key reactive species that may lead to $O_3$ formation, and utilize a model-derived metric to compare relative SOA potentials (Derwent et al., 2010) from each fuel region. Detailed chemical models are required to more accurately account for the various $O_3$ and SOA formation pathways, which is out of the scope of this study. In addition to the laboratory fire measurements, we present field-measurements of rarely-reported VOCs in ambient air during the Fourmile Canyon Fire that affected Boulder, Colorado in September 2010. The latter measurements revealed BB markers that were specific to the BB emissions, minimally influenced by urban or biogenic VOC emission sources, and were emitted in detectable quantities with long enough lifetimes to be useful even in aged, transported BB plumes.

## 2  Experimental

### 2.1  Fuel and biomass burn descriptions

The laboratory-based measurements of BB emissions were conducted in February 2009 at the U.S. Department of Agriculture's Fire Sciences Laboratory in Missoula, Montana. A detailed list of the biomass fuel types, species names, fuel source origin, and the carbon and nitrogen content of the fuels studied here are included in a previous paper by Burling et al. (2010). Up to 5 replicate burns were conducted for each of the 18 different fuels studied. These fuels are categorized into 3 geographic fuel regions based on where the fuels were collected. The data presented here include

9 southwestern fuels from southern California and Arizona including chaparral shrub, mesquite, and oak savanna/woodland; 6 southeastern fuels represented the pine savanna/shrub complexes indigenous to coastal North Carolina and pine litter from Georgia; and 3 northern fuels including an Englemann spruce, a grand fir, and ponderosa pine needles from Montana. All fuels were harvested in January 2009 and sent to the Fire Sciences Laboratory where they were stored in a walk-in cooler prior to these experiments.

All biomass burns were conducted inside the large burn chamber (12.5 m × 12.5 m × 20 m height), which contains a fuel bed under an emissions-entraining hood, an exhaust stack, and an elevated sampling platform surrounding the exhaust stack approximately 17 m above the fuel bed (Christian et al., 2003, 2004; Burling et al., 2010). Each fuel sample was arranged on the fuel bed in a manner that mimicked their natural orientation and fuel loading when possible and was ignited using a small propane torch (Burling et al., 2010). During each fire, the burn chamber was slightly pressurized with outside air conditioned to a similar temperature and relative humidity as the ambient air inside the burn chamber. The subsequent emissions were entrained by the pre-conditioned ambient air and continuously vented through the top of the exhaust stack. The residence time of emissions in the exhaust stack ranged from ∼ 5 to 17 s depending on the flow/vent rate. Each burn lasted approximately 20–40 min from ignition to natural extinction.

## 2.2 Instrumentation and sampling

A list of the gas-phase instruments used in this study, a brief description of their inherent sampling limitations, and references appears in Table 1. The gas chromatograph mass spectrometer (GC-MS) and the proton-transfer-reaction mass spectrometer (PTR-MS) were located in a laboratory adjacent to the burn chamber. The proton-transfer-reaction ion-trap mass spectrometer (PIT-MS), negative-ion proton-transfer chemical-ionization mass spectrometer (NI-PT-CIMS), and open-path Fourier trans-

Biomass burning emissions and potential air quality impacts

J. B. Gilman et al.

Title Page

Abstract | Introduction

Conclusions | References

Tables | Figures

◄ | ►

◄ | ►

Back | Close

Full Screen / Esc

Printer-friendly Version

Interactive Discussion

form infrared (OP-FTIR) optical spectrometer were located on the elevated platform inside the burn chamber.

Sampling inlets for the four mass spectrometers were located on a bulkhead plate on the side of the exhaust stack 17 m above the fuel bed. The GC-MS and PTR-MS shared a common inlet, which consisted of 20 m of unheated 3.97 mm i.d. perfluoroalkoxy Teflon tubing (Warneke et al., 2011). The portion of the inlet line inside the exhaust stack (40 cm) was sheathed by a stainless steel tube (40 cm, 6.4 mm i.d.) that extended 30 cm from the wall of the exhaust stack and was pointing upwards (away from the fuel bed below) in an effort to reduce the amount of particles pulled into the sample line. A sample pump continuously flushed the 25 m sample line with 7 L min$^{-1}$ flow of stack air reducing the inlet residence time to less than 3 s. Separate inlets for both the PIT-MS and NI-PT-CIMS were of similar materials and design, but shorter lengths further reducing inlet residence times and allowing for sample dilution for the NI-PT-CIMS (Roberts et al., 2010; Veres et al., 2010).

The open optical path of the OP-FTIR spanned the full width of the exhaust stack so that the emissions could be measured instantaneously without the use of an inlet. All measurements were time aligned with the OP-FTIR in order to account for different inlet residence times and instrument response times. Previous comparisons of OP-FTIR to a PTR-MS with a moveable inlet confirmed the stack emissions are well-mixed at the height of the sampling platform (Christian et al., 2004). Other possible sampling artifacts, such as losses to the walls of the inlets, were investigated via laboratory tests and in-situ instrument comparisons (Burling et al., 2010; Roberts et al., 2010; Veres et al., 2010; Warneke et al., 2011).

## 2.3 Discrete sampling by in-situ GC-MS

A custom-built, dual-channel GC-MS was used to identify and quantify an extensive set of VOCs. For each biomass burn, the GC-MS simultaneously collected 2 samples, one for each channel, and analyzed them in series using either an $Al_2O_3$/KCl PLOT column (channel 1) or a semi-polar DB-624 capillary column (channel 2) plumbed to a heated

4-port valve that sequentially directed the column effluent to a linear quadrupole mass spectrometer (Agilent 5973N). The sample traps for each channel were configured to maximize the cryogenic trapping efficiencies of high-volatility VOCs (channel 1) or VOCs of lesser volatility and/or higher polarity (channel 2) while minimizing the amount of $O_3$, $CO_2$ and water in each sample (Goldan et al., 2004; Gilman et al., 2010). For each channel, $70\,mL\,min^{-1}$ was continuously sub-sampled from the high volume ($7\,L\,min^{-1}$) sample stream for 20 to 300 s resulting in sample volumes from 23–350 mL each. Smaller sample volumes were often collected during periods of intense flaming combustion in order to avoid trapping excessive $CO_2$, which could lead to dry ice forming in the sample trap, thereby restricting sample flow. Larger sample volumes allowed for detection of trace species, but peak resolution would degrade if the column was overloaded. The mass spectrometer was operated in either total ion mode, scanning all mass-to-charge ratios ($m/z$) from 25 to 150 atomic mass units; or in selective ion mode, scanning a subset of $m/z$'s. The majority of the samples were analyzed in selective ion mode for improved signal-to-noise; however, at least one sample of each fuel type was analyzed in total ion mode to aid identification and quantify species whose $m/z$ may not have been scanned in selective ion mode. The entire GC-MS sampling and analysis cycle required 30 min; therefore, the GC-MS was limited to sampling each laboratory burn only once per fire for burns that lasted less than 30 min. GC-MS samples were collected at different stages of replicate burns in an effort to best characterize the emissions of each fuel type.

Each VOC was identified by its retention time and quantified by the integrated peak area of a distinctive $m/z$ in order to reduce any potential interferences from co-eluting compounds. Identities of new compounds that had never before been measured by this GC-MS were confirmed by (1) matching the associated electron impact ionization mass spectrum when operated in total ion mode to the National Institute of Standards and Technology's mass spectral database, and (2) comparing their respective retention times and boiling points to a list of compounds previously measured by the GC-MS. Examples of these species include: 1,3-butadiyne ($C_4H_2$), butenyne (vinyl acetylene,

C$_4$H$_4$), methylnitrite (CH$_3$ONO), nitromethane (CH$_3$NO$_2$), methyl pyrazole (C$_4$H$_6$N$_2$), ethyl pyrazine (C$_6$H$_8$N$_2$), and tricarbon dioxide (carbon suboxide, C$_3$O$_2$). For some species, we were able to identify the chemical family (defined by its molecular formula and common chemical moiety) but not the exact chemical structure or identity. For these cases, we present the emissions as a sum of the unidentified isomers for a particular chemical family (see Table 2). We report only the compounds that were above the limits of detection for the majority of the biomass burns and where the molecular formula could be identified.

Of the 187 gases quantified by the GC-MS in this study, 95 were individually calibrated with commercially available and/or custom-made gravimetrically-based compressed gas calibration standards. The limit of detection, precision, and accuracy are compound dependent, but are conservatively better than 0.010 ppbv, 15, and 25 %, respectively (Gilman et al., 2009, 2010). For compounds where a calibration standard was not available, the calibration factors were estimated using measured calibrations of compounds in a similar chemical family with a similar retention time, and when possible a similar mass fragmentation pattern. In order to estimate the uncertainty in the accuracy of un-calibrated species, we use measured calibrations of ethyl benzene, o-xylene, and the sum of m- and p-xylenes as a test case. These aromatic species have similar mass fragmentation patterns, are all quantified using $m/z$ 91, and elute within 1 min of each other signifying similar physical properties. If a single calibration factor was used for all these isomers, then the reported mixing ratios could be miscalculated by up to 34 %. We therefore conservatively estimate the accuracy of all un-calibrated species as 50 %.

## 2.4  Calculation of emission ratios

Emission ratios (ER) to carbon monoxide (CO) for each gas-phase compound, $X$, were calculated as follows:

$$\text{ER} = \frac{\Delta X}{\Delta \text{CO}} = \frac{\int_{t_{\text{start}}}^{t_{\text{end}}} (X_{\text{fire}} - X_{\text{bknd}}) \, dt}{\int_{t_{\text{start}}}^{t_{\text{end}}} (\text{CO}_{\text{fire}} - \text{CO}_{\text{bknd}}) \, dt} \tag{1}$$

where $\Delta X$ and $\Delta \text{CO}$ are the excess mixing ratios of compound $X$ or CO, respectively, during a fire above the background. Background values, $X_{\text{bknd}}$ and $\text{CO}_{\text{bknd}}$, are equal to the average mixing ratio of a species in the pre-conditioned ambient air inside the exhaust stack in the absence of a fire. For the OP-FTIR, PTR-MS, PIT-MS and NI-PT-CIMS, backgrounds were determined from the mean responses of the ambient air inside the exhaust stack for a minimum of 60 s prior to the ignition of each fire. At least one background sample was collected for the GC-MS each day. The composition and average mixing ratios of VOCs in the stack backgrounds were consistent over the course of the campaign and were generally much lower than the mixing ratios observed during biomass burns. For example, the average background ethyne measured by the GC-MS was $1.22 \pm 0.33$ ppbv (median $= 1.21$ ppbv) compared to a mean ethyne of $150 \pm 460$ ppbv (median $= 42$ ppbv) in the fires. The large standard deviation for ethyne in the biomass burns reflects the large variability in ethyne emissions rather than uncertainty in the measurement.

The type of emission ratio, discrete or fire-integrated, is determined by the sampling frequency of the instrument and sampling duration. The GC-MS is only capable of measuring discrete ERs, which represent the average $\Delta X$ relative to $\Delta \text{CO}$ for a relatively short portion of a fire corresponding to the GC-MS sample acquisition time. The OP-FTIR, PTR-MS, and NI-PT-CIMS are fast-response instruments that sampled every 1 to 10 s over the entire duration of each fire. These measurements were used to calculate both fire-integrated ERs that represent to $\Delta X / \Delta \text{CO}$ over the entirety of a fire ($dt \geq 1000$ s) (Burling et al., 2010; Veres et al., 2010; Warneke et al., 2011) as well

as discrete ERs coincident with the GC-MS sample acquisition (d$t$ = 20 to 300 s) as discussed in Sect. 2.3. We reference all ERs to CO because the majority of VOCs and CO are co-emitted by smoldering combustion during the fire whereas $CO_2$ emissions occur mostly from flaming (see Sect. 3.1). Additionally, ratios to CO are commonly reported in the literature for biomass burning and urban VOC emission sources. All data presented here are in units of ppbv VOC per ppmv CO, which is equivalent to a molar ratio (mmol VOC (mol CO)$^{-1}$).

## 2.5  Fourmile Canyon Fire in Boulder, Colorado

Ambient air measurements of biomass burning emissions from the Fourmile Canyon Fire that occurred in the foothills 10 km west of Boulder, Colorado were conducted from 7–9 September 2010. Over the course of the Fourmile Fire, approximately 25 km$^2$ of land including 168 structures burned. The burned vegetation consisted primarily of Douglas-fir (*Pseudotsuga menziesii*) and ponderosa pine (*Pinus ponderosa*) mixed with juniper (*Juniperius scopulorum* and *communis*), mountain mahogany (*Cercocarpus*), and various shrubs and grasses common to the mountain zone of the Colorado Front Range (Graham et al., 2012). During the measurement period, down-sloping winds ranging from 1 to 12 m s$^{-1}$ (mean = 3.5 m s$^{-1}$) periodically brought biomass burning emissions to NOAA's Earth Systems Research Laboratory located at the western edge of the city of Boulder. The previously described in-situ GC-MS was housed inside the laboratory and sampled outside air via a 15 m Teflon sample line (residence time < 2 s) attached to an exterior port on the western side of the building. CO was measured via a co-located vacuum-UV resonance fluorescence instrument (Gerbig et al., 1999).

**Biomass burning emissions and potential air quality impacts**

J. B. Gilman et al.

## 3   Results and discussion

### 3.1   Calculation of emission ratios

Temporal profiles of laboratory biomass burns provide valuable insight into the combustion chemistry and processes that lead to the emissions of various species (Yokelson et al., 1996). Figure 1 shows temporal profiles of an example burn in order to illustrate (i) flaming, mixed, and smoldering combustion phases/processes and (ii) the sampling frequencies and temporal overlap of the fast-response instruments compared to the GC-MS. Upon ignition, there is an immediate and substantial increase in $CO_2$ and $NO_x$ ($NO + NO_2$) indicative of vigorous flaming combustion. This transitions to a mixed-phase characterized by diminishing $CO_2$ and $NO_x$ emissions and a second increase in CO. The fire eventually evolves to a weakly-emitting, protracted period of mostly smoldering combustion (Yokelson et al., 1996; Burling et al., 2010). Figure 1 also includes the temporal profile of the modified combustion efficiency, $MCE = \Delta CO_2/[\Delta CO + \Delta CO_2]$, which is a proxy for the relative amounts of flaming and smoldering combustion (Yokelson et al., 1996). During the initial flaming phase of the fire, the MCE approaches unity due to the dominance of $CO_2$ emissions. The MCE gradually decreases during smoldering combustion when CO emissions are more prominent.

In order to compare measurements from multiple instruments, we calculated the average excess mixing ratios of a species, $\Delta X$, measured by the fast-response instruments over the corresponding GC-MS sample acquisition times for all 56 biomass burns. We compare the measurements using correlation plots of $\Delta X$ for VOCs measured by the GC-MS vs. the same compound measured by the OP-FTIR or an analogous $m/z$ measured by the PTR-MS. The slopes and correlation coefficients, $r$, were determined by linear orthogonal distance regression analysis and are compiled in Fig. 2a. The average slope and standard deviation of the instrument comparison is $1.0 \pm 0.2$ and $0.93 < r < 0.99$ signifying good overall agreement between the different

measurement techniques for the species investigated here. A few comparisons are discussed in more detail below.

The largest difference between the GC-MS and the OP-FTIR observations was for propene (slope = 1.36) indicating that the GC-MS response is greater than the OP-FTIR; however, a correlation coefficient of 0.99 suggests that the offset is more likely from a calibration difference that remains unresolved. The possibility of a species with the same retention time and similar fragmentation pattern as propene that is also co-emitted at a consistent ratio relative to propene seems highly unlikely, but cannot be completely ruled out. For furan, the GC-MS had a lower response than OP-FTIR (slope = 0.77) indicating that the GC-MS may be biased low for furan or that the OP-FTIR may have spectral interferences that bias the measurement high. The temporal profiles of these measurements shown in Fig. 1 suggest that there was a spectral interference with the OP-FTIR measurement of furan as evidenced by the large emissions in the flaming phase that was not captured by the $m/z$ 69 response of the PTR-MS. These early "spurious" OP-FTIR furan responses would (i) only affect the comparison for the GC-MS samples collected in the flaming phase of the fires and (ii) have not been observed in other biomass burning experiments utilizing this OP-FTIR (Christian et al., 2004; Stockwell et al., 2014).

Comparison of the GC-MS Σ (isoprene + furan) vs. PTR-MS $m/z$ 69 has the lowest slope (GC-MS vs. PTR-MS = 0.64) indicating the contribution of other VOCs, e.g. cis- and trans-1,3-pentadienes, to the $m/z$ 69 response of the PTR-MS in fresh smoke (Warneke et al., 2011). Carbon suboxide ($C_3O_2$) has also been shown to contribute to $m/z$ 69 response for the PTR-MS technique (Stockwell et al., 2015). Direct comparisons of the real-time measurements for a variety of other species not measured by the GC-MS (e.g., formaldehyde, formic acid, and HONO) can be found elsewhere (Burling et al., 2010; Veres et al., 2010; Warneke et al., 2011).

## 3.2 Comparison of discrete and fire-integrated ERs

Fire-integrated ERs represent emissions from all combustion processes of a biomass burn whereas discrete ERs capture a relatively brief snapshot of emissions from mixed combustion processes during a particular sampling period. Figure 1 includes time series of VOC to CO ERs measured by the real-time measurement techniques for select gases. Here we compare the 2 different measurement strategies, discrete vs. fire-integrated, in order to (i) determine if the discrete ERs measured by the GC-MS may be biased by the sample acquisition times which typically occurred within the first-half of a laboratory burn when emissions for most gases generally "peaked" and (ii) assess how well the discrete GC-MS samples are able to capture the fire-to-fire variability of emissions relative to CO. We do this by determining discrete ERs for the OP-FTIR or PTR-MS for each of the 56 biomass burns using Eq. (1) where $t_{start}$ and $t_{end}$ times correspond to the GC-MS sample acquisition. The discrete ERs are then compared to the fire-integrated ERs measured by the same fast-response instrument so that potential measurement artifacts will not affect the comparison.

The slopes and correlation coefficients, $r$, of discrete vs. fire-integrated ERs for select VOCs are summarized in Fig. 2b. These values were calculated using a linear orthogonal distance regression analysis of correlation plots of discrete vs. fire-integrated ERs as shown in Fig. 3. The average slope and standard deviation is $1.2 \pm 0.2$ indicating that the discrete ERs are generally higher than the fire-integrated ERs by 20 % on average. This positive bias is a consequence of the GC-MS sampling strategy which rarely included samples collected at the end of a burn (e.g., $t \geq 1000\,s$ in Fig. 1) when absolute emissions and ERs are lower for most species. Using the data in Fig. 1 as an example, 95 % of the emissions of benzene (in ppbv) occur between ignition and 1000 s, and the mean ER during this time is twice as large as the mean ER in the later portion of the fire (time = 1001 s to extinction). For VOCs emitted during the later stages of a fire (e.g., 1,3-benzenediol), the discrete ERs will likely underestimate the emissions relative to CO. For example, the discrete ERs for benzenediol for the southeastern and south-

Title Page

Abstract | Introduction

Conclusions | References

Tables | Figures

|◄ | ►|

◄ | ►

Back | Close

Full Screen / Esc

Printer-friendly Version

Interactive Discussion

western fuels (Table 2) are 30 % lower than the mean fire-integrated ERs reported by Veres et al. (2010).

The ability of the GC-MS to capture the fire-to-fire variability in VOC emissions relative to CO is evaluated by the strength of the correlation, $r$, between the discrete and fire-integrated ERs (Fig. 2b). Species with the weakest correlations, such as ethyne and benzene, show a distinct bifurcation that is dependent upon the MCE of the discrete samples (Fig. 3). These compounds have significant portion of emissions in both the flaming and smoldering phases of a fire (see Fig. 1). For these types of compounds, discrete samples collected in the smoldering phase (low MCE) did not adequately represent the fire-integrated emissions that include the intense flaming emissions (high MCE) resulting in poor correlation between discrete and fire-integrated ERs for these species. In contrast, VOCs that had the strongest correlations between the discrete and fire-integrated ERs (e.g., methanol and toluene where $r > 0.88$) do not show a strong dependence on the MCE. Since CO is strongly associated with smoldering combustion (Yokelson et al., 1996; Burling et al., 2010), VOCs emitted primarily during this phase will be more tightly correlated with CO and the variability in the discrete vs. fire-integrated will be minimized.

In summary, the discrete GC-MS samples best characterize the fire-integrated emissions and fire-to fire variability of species produced primarily by smoldering combustion. We conservatively estimate these values to be within a factor of 1.5 of the fire-integrated ERs for the majority of the species measured. A similar conclusion was reached by comparing discrete ERs measured during the same fire to each other by Yokelson et al. (2013). While fire-integrated ERs are considered to best represent BB emissions, these analyses suggest that collecting and averaging multiple discrete ERs at various stages of the same or replicate burns, as presented here, are an adequate substitute when fire-integrated ERs cannot be determined. Fire-integrated ERs are commonly used to determine fuel-based emission factors for a fire, but care must be taken converting discrete ERs into emission factors, as also discussed for this data in Yokelson et al. (2013).

## 3.3 Characterization of laboratory BB emissions

In order to merge datasets from multiple instruments, we report mean discrete ERs of over 200 organic gases, including methane and VOCs, and 9 inorganic gases relative to CO for the southwestern, southeastern, and northern fuel types in the United States (Table 2). Mean ERs for each of the 18 individual fuel types are available at http://www.esrl.noaa.gov/csd/groups/csd7/measurements/2009firelab/. This study utilizes discrete ERs to characterize the chemical composition of the molar mass emitted, the VOC-OH reactivity, and the SOA potential of the measured emissions from fires simulating each fuel region in order to compare potential atmospheric impacts of these emissions and identify key species that may impact air quality through formation of $O_3$ and/or SOA.

Figure 4 is a pictograph of all ERs presented in Table 2 as well as a histogram of the ERs for each of the 3 fuel regions in order to highlight commonalities and differences in the magnitudes and general chemical composition of each simulated fuel region. The distribution of ERs are shown as a function of three simple properties including the degree of unsaturation ($D = [2C + N - H + 2]/2$, where C, N, and H denote the number of carbon, nitrogen, and hydrogen atoms, respectively); the number of oxygen atoms; and molecular weight (MW) of individual VOCs. Atmospheric lifetimes and fates of VOCs will depend, in part, on these properties, which we use as simplified proxies for reactivity (D), solubility (O-atoms), and volatility (MW). Using this general framework, we highlight several key features that will be explored in further detail in the subsequent sections:

i. ERs are highly variable and span more than 4 orders of magnitude.

ii. The relative magnitude and composition of the gases emitted are different for each of the 3 geographic fuel regions, i.e., the distribution of ERs are unique to each fuel region.

iii. Southwestern fuels generally have lower ERs and northern fuels have the largest ERs. Collectively, the molar emission ratios are a factor of 3 greater for the northern fuels than the southwestern.

iv. The largest ERs for all three fuel regions are associated with low molecular weight species (MW < 80 g mol$^{-1}$) and/or those that contain 1 or more oxygen atom(s). These species also have lower degrees of unsaturation ($D \leq 2$) and populate the upper left quadrants of Fig. 4. VOCs with the largest ERs common to all fuel types are formaldehyde, ethene, acetic acid, and methanol (Table 2).

v. Over 82 % of the molar emissions of VOCs from biomass burning are unsaturated compounds ($D \geq 1$) defined as having one or more pi-bonds (e.g., C-C or C-O double bonds, cyclic or aromatic rings, etc.). In general, these species are more likely to react with atmospheric oxidants and/or photo-dissociate depending on the chemical moiety, making unsaturated species potentially important $O_3$ and SOA precursors. VOCs that contain triple bonds (e.g., ethyne) are a notable exception as they tend to be less reactive.

vi. The number of VOCs in the upper right quadrants of Fig. 4 (increasing ERs and degree of unsaturation) is greatest for northern fuels and least for southwestern fuels. Many of the VOCs in this quadrant also have relatively high molecular weights (MW $\geq$ 100 g mol$^{-1}$) and most contain at least one oxygen atom (e.g., benzenediol and benzofuran). The combination of these physical properties indicate that these species are relatively reactive, soluble, and of low enough volatility to make them potentially important SOA precursors.

### 3.3.1 Molar mass emitted

Here we compare the magnitude and composition of biomass burning emissions as a function of molar mass, which is a readily calculated physical property used to quan-

tify BB emissions. Molar mass ($\mu g\,m^{-3}$) emitted per ppmv CO is equal to:

$$\text{Molar Mass} = \sum \left( \frac{\text{ER} \cdot \text{MW}}{\text{MV}} \right) \tag{2}$$

where ER is the mean discrete emission ratio of a gas, MW is the molecular weight ($g\,mol^{-1}$), and MV is molar volume (24.5 L at 1 atm and 25 °C). For all 3 fuel regions, $CO_2$ was the overwhelmingly dominant gas-phase emission and singularly contributed over 95 % of the molar mass emitted. Collectively, $CH_4$ and the inorganic gases (e.g., $CO_2$, CO, $NO_x$, etc.) comprised over 99.05 % of all gaseous molar mass emitted and measured, while VOCs contributed only $0.27 \pm 0.03$, $0.34 \pm 0.03$, and $0.95 \pm 0.07$ % for the southeastern, southwestern, and northern fuels, respectively.

Figure 5a–c shows the fractional composition and total molar mass of measured VOCs emitted per ppmv CO for each fuel region. The molar mass emitted by northern fuels ($324 \pm 22\,\mu g\,m^{-3}\,ppmv\,CO^{-1}$) is 3.5 times greater than the southwestern fuels ($92 \pm 9\,\mu g\,m^{-3}\,ppmv\,CO^{-1}$). For all 3 fuel regions, the emissions are dominated by oxygen-containing VOCs (OVOCs), which collectively comprise 57–68 % of the total mass emissions. The largest contribution by a single chemical class is from OVOCs with low degrees of unsaturation ($D \leq 1$), which contribute 29–40 % of the total molar mass emitted. This chemical family is dominated by acetic acid, formaldehyde, and methanol emissions (Table 2). Compared to hydrocarbons and OVOCs, nitrogen-containing VOCs are emitted in substantially smaller fractions, less than 8 % of the total. Dominant nitrogen VOCs include hydrocyanic acid (HCN), isocyanic acid (HNCO), acetonitrile ($CH_3CN$), and methylnitrite ($CH_3ONO$). The addition of all nitrogen-containing organics presented here would add approximately 5 % to the nitrogen budget presented in Burling et al. (2010); however, this would still leave over half of the fuel nitrogen potentially ending up in the ash, or being emitted as $N_2$ or in other unmeasured gases based on the nitrogen content of the fuels which ranged from 0.48 to 1.3 %.

One limitation of this analysis is the exclusion of "unknown" species, which are (i) gaseous compounds that were measured but remain unidentified and were therefore omitted from this analysis because the chemical formula and family could not be properly identified or (ii) were undetectable by the suite of instruments listed in Table 1. We estimate the mass contribution from the first scenario using the fuel-based emission factors compiled by Yokelson et al. (2013) for all measured species including "unknown" masses observed by the PIT-MS. These "unidentified" non-methane organic compounds (NMOC, equivalent to VOCs) accounted for 31–47 % of the mass emitted for the same fuels studied here (Yokelson et al., 2013). The second category of unobserved unknown species are likely to be of sufficiently high molecular weight, high polarity, and/or low volatility and thermal stability to escape detection by GC-MS, a variety of chemical ionization mass spectrometers, and the OP-FTIR. For example, BB emissions of species such as glyoxal, glycoaldehyde, acetol, guaiacols, syringols, and amines have been reported in the literature (McDonald et al., 2000; Schauer et al., 2001; McMeeking et al., 2009; Akagi et al., 2011, 2012; Hatch et al., 2015) but would not be detectable by any of the instruments used in this experiment. The contribution of these types of compounds is difficult to assess, so we roughly estimate an additional contribution of $\sim$ 5 % to the total mass emitted could be from un-observed unknown VOCs. Collectively, we estimate that the species reported in Table 2 and compiled in Fig. 5a–c account for approximately 48–64 % of the expected mass of non-methane organic gases emitted from the fuels studied here. The total VOC molar mass emitted for each fuel type should be considered a lower limit and could increase by a factor of $\sim$ 2. By extension, all of the totals presented in Fig. 5 should also be considered lower limits; however, the additional contribution of unidentified and/or un-measured species to the following discussions could not be determined.

### 3.3.2 OH reactivity of BB emissions

Oxidation of VOCs, often initiated by reaction with the hydroxyl radical ($\bullet$OH), in the presence of $NO_x$ ($NO + NO_2$) leads to the photochemical formation of $O_3$ and perox-

ynitrates, including peroxyacetic nitric anhydride (PAN). Due to the complex relationship between $O_3$ production and VOC/$NO_x$ ratios and peroxynitrates, we use OH reactivity as a simplified metric to (i) compare the magnitude of reactive gases emitted by combustion of fuels characteristic of each region and to (ii) identify key reactive species that may contribute to the photochemical formation of $O_3$ in a BB plume. Total OH reactivity represents the sum of all sinks of the hydroxyl radical (•OH) with all reactive gases and is equal to:

$$OH\,reactivity = \sum (ER \cdot k_{OH} \cdot A) \tag{3}$$

where ER is the discrete emission ratio for each measured gases (VOCs, $CH_4$, CO, $NO_2$, and $SO_2$; $ppbv\,(ppm\,CO)^{-1}$), $k_{OH}$ is the first-order reaction rate coefficient of a gas with the hydroxyl radical ($cm^3\,molec^{-1}\,s^{-1}$), and $A$ is a molar concentration conversion factor ($2.46 \times 10^{10}\,molec\,cm^{-3}\,ppbv^{-1}$ at 1 atm and 25 °C). Reaction rate coefficients were compiled using the National Institute of Standards and Technology's Chemical Kinetics Database and the references therein (Manion et al., 2015). Based on the calculated OH reactivities of all measured species listed in Table 2, VOCs are the dominant sink of OH for all fuel regions contributing 70–90 (±16) % of the total calculated OH reactivity even though non-methane VOCs were only 0.27–0.95 % of the molar mass emitted.

Figure 5d–f shows the fractional contributions and total VOC-OH reactivities per ppmv CO for each of the 3 fuel regions. The fresh BB emissions from northern fuels have the highest OH reactivity ($62 \pm 10\,s^{-1}$ ppmv $CO^{-1}$), which is 4.4 times greater than southwestern fuels ($14 \pm 3\,s^{-1}$ ppmv $CO^{-1}$). Collectively, OVOCs provide the majority of the OH reactivity of the southeastern fuels (57 %), while hydrocarbons dominate the southwestern (52 %) and northern fuels (56 %). Northern fuels have the largest contribution from highly reactive terpenes (14 %) due to the ERs of these species being, on average, a factor of 5 greater than southeastern fuels and a factor of 40 greater than southwestern fuels.

**Biomass burning emissions and potential air quality impacts**

J. B. Gilman et al.

Title Page

| Abstract | Introduction |
| Conclusions | References |
| Tables | Figures |

◀ | ▶|

◀ | ▶

Back | Close

Full Screen / Esc

Printer-friendly Version

Interactive Discussion

For all 3 fuel regions, alkenes have the largest contribution of any singular chemical class due to the large ERs of the reactive species ethene and propene, the latter of which is the single largest individual contributor to OH reactivity of any species measured. Oxidation of alkenes proceeds by OH addition to the double-bond or hydrogen abstraction and often results in the secondary formation of carbonyls (e.g., acetaldehyde and acetone), which are important peroxynitrate precursors (Roberts et al., 2007; Fischer et al., 2014). Primary emissions of formaldehyde is the second-largest contributor, after propene, to the OH reactivity of all VOCs emitted for all 3 fuel regions. Formaldehyde is reactive with OH and is a photolytic source of RO• radicals that also contribute to $O_3$ formation, in addition to being an air toxic.

Other important contributions to OH reactivity of BB emissions include highly unsaturated OVOCs (e.g., 2-propenal, methyl vinyl ketone, and methacrolein), poly-unsaturated alkenes (e.g., 1,3-butadiene and 1,3-cyclopentadiene), and furans. The majority of these types of species are highly reactive with a variety of oxidants and many of their oxidation products are photochemically active. For example, oxidation of 1,3-butadiene results in highly reactive OVOC products including furans and 2-propenal, a precursor of peroxyacrylic nitric anhydride (APAN) (Tuazon et al., 1999). The OH reactivity of furans is dominated by 2-methylfuran, 2-furaldehyde (2-furfural), and furan. Alkyl furans have reaction rate coefficients on the order of $\sim 1 \times 10^{-10}\ cm^3\ molec^{-1}\ s^{-1}$ at 298 K roughly equivalent to that of isoprene and the major oxidation products include dicarbonyls (Bierbach et al., 1992, 1995; Alvarez et al., 2009). Up to 27 furan isomers have been identified from the combustion of Ponderosa Pine (Hatch et al., 2015), indicating this is an important class of species that should be further explored in order to better determine their potential contributions to $O_3$ and SOA formation.

Nitrogen-containing VOCs contribute less than 4 % of the OH reactivity of all fuels due to the low reactivities of the most abundant emissions, which often contain –C≡N functional groups. Some nitriles, such as acetonitrile ($CH_3CN$), can have lifetimes on the order of months making these species good markers of long-range transport of

BB plumes (Holzinger et al., 1999; de Gouw et al., 2003, 2006). Other more reactive nitrogen-containing organics including 2-propenenitrile, benzonitrile, and heterocyclic species such as pyrroles could serve as BB markers of fresh plumes (Friedli et al., 2001; Karl et al., 2007).

### 3.3.3 SOA potential of BB emissions

VOCs that are efficient SOA precursors are relatively reactive organic compounds whose oxidation products are of sufficiently low volatility or high solubility under some conditions. Aerosol yield is a measure of the mass of condensable compounds created from this oxidation per mass of VOC precursor; however, care must be taken to ensure that aerosol yields for various species were determined under comparable conditions (e.g., $VOC:NO_x$ ratios, oxidant concentrations, etc.). In order to conduct comparisons of SOA potential on a consistent scale, we use a model-based unitless metric developed by Derwent et al. (2010) that "reflects the propensity of VOCs to form SOA on an equal mass basis relative to toluene". The photochemical transport model used to investigate SOA potentials (SOAPs) of 113 VOCs included explicit chemistry from the Master Chemical Mechanism (MCM v 3.1) using an idealized set of atmospheric conditions typical of a polluted urban boundary layer (Derwent et al., 2010). SOAPs were determined by the simulated mass of aerosol formed per mass of VOC reacted and is expressed relative to toluene (SOAP = 100). Species such as styrene and benzaldehyde have SOAP values of $\sim 200$ (i.e., twice as much potential SOA formed compared to toluene) and were used to estimate SOAPS for aromatics with unsaturated substituents, benzofurans, and benzenediols.

Figure 5g–i shows the composition and mean SOAPs of VOCs emitted for each of the 3 fuel regions. Southwestern fuels have the lowest SOA potential (480 per ppmv CO) compared to southeastern and northern fuels that have estimated SOAPs 2.7 and 5.1 times greater, respectively. Unsaturated OVOCs are the dominant fraction for all three fuel regions due to the relatively large ERs and SOAPs of benzenediols (sum of 1,2- and 1,3-), benzaldehyde, and phenols. Schauer et al. (2001) reports signifi-

cant gaseous emissions of benzenediols from combustion of pine in a fireplace and shows that 1,2-benzenediol (o-benzenediol) is the dominant gas-phase isomer while 1,3-benzenediol (m-benzenediol) is primarily associated with the particle phase. The discrete ERs used in this comparison may underestimate the emissions and SOA contribution of several compounds emitted in the later portions of a laboratory burn when emissions of most VOCs and CO were lower as previously discussed (Sect. 3.2).

The largest contributions to SOAP from hydrocarbons include aromatics with saturated functional groups (if any) such as benzene and toluene and aromatics with unsaturated substituents such as styrene. Traditionally, these are the species that are thought to be the largest contributors to SOA formation from urban emissions (Odum et al., 1997; Bahreini et al., 2012), although predicted SOA is typically much lower than observed in ambient air suggesting that the aerosol yields may be too low or there are additional SOA precursors that remain unaccounted for (de Gouw et al., 2005).

Monoterpenes have a very small (< 2 %) contribution to total SOAP. The calculated SOAPs of monoterpenes are only 20 % that of toluene (Derwent et al., 2010). This is in contrast to measured aerosol yields which are approximately 1.7 times higher for monoterpenes compared to toluene (Pandis et al., 1992). As a sensitivity test, we increased the SOAPs of the monoterpenes by a factor of 10 bringing the SOAP ratio of monoterpenes to toluene in line with that of measured aerosol yields. This resulted in modest increases in total SOAP of only 2 % for SW and 5 % for SE fuels. N fuels had the largest increase in total SOAP at 16 %. With the adjusted monoterpene SOAPs, the fractional contribution of terpenes increased from 1.8 % (Fig. 5i) to 15 % of the total SOAP while the contribution of unsaturated OVOCs remained the dominant class but was reduced from 67 to 58 % of the total SOAP. This sensitivity test suggests that the contributions of monoterpenes are likely underestimated for northern fuels if the SOAP scale is used; however, the largest contributions to SOAP for the northern fuels continues to be from oxygenated aromatics (benzenediols, phenols, and benzaldehyde). For comparison, Hatch et al. (2015) estimated that the SOA mass formed from the combustion of Ponderosa Pine is dominated by aromatic hydrocarbons (45 %), terpenes

(25 %), phenols (9 %), and furans (9 %); however, their analysis did not include contributions from benzenediols (not measured), benzaldehyde or benzofurans (measured but not included in estimate).

## 3.4 Field measurements of BB emissions

Here we present field-measurements of VOCs in ambient air during the Fourmile Canyon Fire that affected Boulder, Colorado in September 2010. The in-situ GC-MS measurements are shown in Fig. 6 and summarized in Table 3. We were able to identify and quantify a number of VOCs in ambient BB plumes that we had only previously observed in the fire emissions at the Fire Sciences Laboratory. Analysis of BB plumes from the Fourmile Canyon Fire afforded a unique opportunity to investigate BB emissions measured by this same GC-MS system in simulated and real fires and to explore issues associated with the presence of other VOC sources such as urban emissions and natural biogenic emissions during both the daytime and nighttime; with nighttime smoke measurements being very rarely reported (Adler et al., 2011).

First we identify the potential emission sources impacting the measurements. Acetonitrile is a common BB tracer that we use to help clarify periods of BB influence. As seen in Fig. 6, BB plumes are readily distinguished by concurrent increases in acetonitrile ($CH_3CN$), carbon monoxide (CO), and several VOCs. Species such as benzonitrile and furan are very tightly correlated with acetonitrile ($r > 0.94$, Table 3) and enhancements in ambient mixing ratios above detection limit only occur in the BB plumes indicating that BB was the only significant source of these compounds. VOCs such as isoprene and alpha-pinene were similarly enhanced in the BB plumes and well correlated with acetonitrile during BB episodes; however, the mixing ratios observed in the BB plume were generally lower than those observed at other times from the natural sunlight-dependent emissions of isoprene (e.g., 09:00–15:00 LT) and from the accumulation of monoterpenes in the nocturnal boundary layer (e.g., 9 August 2010 18:00 to 9 September 2010 06:00 LT). 3-Carene was the only monoterpene that had significantly higher mixing ratios in the BB plume than in biogenic emissions. Ethene, ethyne,

benzene, styrene, and methanol were enhanced in the BB plumes but are also present in urban emissions. An urban plume at 06:00–09:00 LT 9 September 2010 (Fig. 6) is enhanced in all of these species and CO; however, acetonitrile is not enhanced.

Observed enhancement ratios of several VOCs relative to acetonitrile and CO are compiled in Table 3 along with the types of emission sources for each VOC. Figure 7 shows a comparison of the VOC to acetonitrile ratios of select species for the Fourmile Canyon Fire and the laboratory-based biomass burns of all fuel types. We have identified benzofuran, 2-furaldehyde, 2-methylfuran, furan, and benzonitrile as the "best" tracers for BB emissions from these observations. These species (i) were well correlated with both acetonitrile and CO in the BB plumes, (ii) had negligible emissions from the urban and biogenic sources impacting the measurement site, and (iii) had large enhancements in BB plumes. In theory, the relative ratios of these species to acetonitrile may also be used as a BB-specific photochemical clock since each of these species represent a range of reactivities that are much greater than that of acetonitrile (Table 3). We compared the enhancement ratios of each VOC marker vs. acetonitrile for the two BB plumes observed on 9 August 2010 in order to determine if the relative age of the two BB plumes could be distinguished. While the enhancement ratios for several VOCs in each plume were statistically different from one another, there was no clear relationship between the observed differences in the enhancement ratios and the relative reactivity of the VOCs. Thus, small differences in the observed enhancement ratios more likely relate to differences in the fuel composition, the relative ratio of flaming vs. smoldering emissions in each BB plume, or variable secondary sources. Given enough time for significant photochemistry to occur as a BB plume moves further from the source, these ratios could be more useful to estimate photochemical ages.

## 4   Conclusions

We report a chemically detailed analysis of the trace gases emitted from burning 18 different biomass fuel types important in the southwestern, southeastern, and northern

Title Page

Abstract   Introduction

Conclusions   References

Tables   Figures

Back   Close

Full Screen / Esc

Printer-friendly Version

Interactive Discussion

US. A complementary suite of state-of-the-art instruments was used to identify and quantify over 200 organic and 9 inorganic gases emitted from laboratory burns. Most of the species were quantified via discrete sampling by the GC-MS, which also provided confirmation for the real-time PIT-MS and PTR-MS mass assignments (Warneke et al., 2011). The variability in emissions over the course of each biomass burn was measured in detail by the fast-response instruments providing valuable insight into the combustion chemistry and processes that govern the emissions of various species.

By comparing discrete and fire-integrated ERs for various VOCs relative to CO, we show that the discrete GC-MS samples adequately represented the fire-integrated ER within an average factor of $1.2 \pm 0.2$ and fire-to-fire variability for VOCs emitted mainly by smoldering, which are the majority of VOCs. Discrete ERs for VOCs emitted by both flaming and smoldering were highly variable and showed a clear bifurcation depending on the mix of combustion processes during sampling. This analysis highlights the importance of collecting multiple discrete samples at various stages of replicate burns if fire-integrated emissions cannot be measured to ensure adequate measurement of all VOCs.

The distribution of VOC emissions (magnitude and composition) was different for each fuel region. The largest total VOC emissions were from fuels representing the northern U.S. while southwestern U.S. fuels produced the lowest total VOC emissions. VOCs contributed less than $0.78 \pm 0.12\%$ of total detected gas-phase emissions by mole and less than $0.95 \pm 0.07\%$ by mass due to the predominance of $CO_2$, CO, $CH_4$, and $NO_x$ emissions. However, VOCs contributed 70–90 ($\pm16$) % of the total calculated OH reactivity and 100 % of the potential SOA precursors emitted from combustion of biomass. Over 82 % of the VOC emissions by mole are unsaturated species including highly reactive alkenes, aromatics and terpenes as well as photolabile OVOCs such as aldehydes and ketones. VOCs with the largest ERs common to all fuel types are formaldehyde, ethene, acetic acid, and methanol.

OVOCs contributed the dominant fraction of both the total VOC mass emitted (> 57 %) and potential SOA precursors (> 52 %), and also contributed a significant

fraction of the OH reactivity for all fuel regions making them an important class of VOCs to understand the air quality impacts of BB emissions. Reactive and photolabile OVOCs such as formaldehyde, 2-propenal (acrolein), and 3-butenal (crotonaldehyde) are toxic, a source of free radicals, and/or precursors of peroxynitrates that may con-
tribute to $O_3$ formation downwind of the source. Furans are a class of OVOCs in BB emissions that contributed more than 14 % of the OH reactivity for all fuel regions; however, their potential as SOA precursors, particularly for species such as 2-furaldehyde and benzofuran, requires further study. The estimated SOA potential was dominated by oxygenated aromatics (benzenediols, phenols, and benzaldehyde). Potentially impor-
tant species that were not measured but should be considered in future studies include glyxoal, glycoaldehyde, acetol, guaiacols, and syringols (Stockwell et al., 2015).

The Fourmile Canyon Fire in Boulder, CO, allowed us to identify and quantify a number of VOCs in ambient BB plumes that we had only previously observed in the emissions from laboratory fires at the Fire Sciences facility and investigate BB emissions
in the presence of other VOC sources such as urban emissions and biogenic emissions during both the day and nighttime. We identified benzofuran, 2-furaldehyde, 2-methylfuran, furan, and benzonitrile as the "best" tracers for BB emissions from our observations. In theory, the relative ratios of these species to acetonitrile may also be used as a BB-specific photochemical clock since each of these species represent
a range of reactivities assuming a negligible photochemical source.

**ACPD**

15, 21713–21763, 2015

**Biomass burning emissions and potential air quality impacts**

J. B. Gilman et al.

# References

Adler, G., Flores, J. M., Abo Riziq, A., Borrmann, S., and Rudich, Y.: Chemical, physical, and optical evolution of biomass burning aerosols: a case study, Atmos. Chem. Phys., 11, 1491–1503, doi:10.5194/acp-11-1491-2011, 2011.

Akagi, S. K., Yokelson, R. J., Wiedinmyer, C., Alvarado, M. J., Reid, J. S., Karl, T., Crounse, J. D., and Wennberg, P. O.: Emission factors for open and domestic biomass burning for use in atmospheric models, Atmos. Chem. Phys., 11, 4039–4072, doi:10.5194/acp-11-4039-2011, 2011.

Akagi, S. K., Craven, J. S., Taylor, J. W., McMeeking, G. R., Yokelson, R. J., Burling, I. R., Urbanski, S. P., Wold, C. E., Seinfeld, J. H., Coe, H., Alvarado, M. J., and Weise, D. R.: Evolution of trace gases and particles emitted by a chaparral fire in California, Atmos. Chem. Phys., 12, 1397–1421, doi:10.5194/acp-12-1397-2012, 2012.

Alvarado, M. J. and Prinn, R. G.: Formation of ozone and growth of aerosols in young smoke plumes from biomass burning: 1. Lagrangian parcel studies, J. Geophys. Res.-Atmos., 114, D09306, doi:10.1029/2008jd011144, 2009.

Alvarado, M. J., Lonsdale, C. R., Yokelson, R. J., Akagi, S. K., Coe, H., Craven, J. S., Fischer, E. V., McMeeking, G. R., Seinfeld, J. H., Soni, T., Taylor, J. W., Weise, D. R., and Wold, C. E.: Investigating the links between ozone and organic aerosol chemistry in a biomass burning plume from a prescribed fire in California chaparral, Atmos. Chem. Phys., 15, 6667–6688, doi:10.5194/acp-15-6667-2015, 2015.

Alvarez, E. G., Borras, E., Viidanoja, J., and Hjorth, J.: Unsaturated dicarbonyl products from the OH-initiated photo-oxidation of furan, 2-methylfuran and 3-methylfuran, Atmos. Environ., 43, 1603–1612, doi:10.1016/j.atmosenv.2008.12.019, 2009.

Andreae, M. O. and Merlet, P.: Emission of trace gases and aerosols from biomass burning, Global Biogeochem. Cy., 15, 955–966, 2001.

Bahreini, R., Middlebrook, A. M., de Gouw, J. A., Warneke, C., Trainer, M., Brock, C. A., Stark, H., Brown, S. S., Dube, W. P., Gilman, J. B., Hall, K., Holloway, J. S., Kuster, W. C., Perring, A. E., Prevot, A. S. H., Schwarz, J. P., Spackman, J. R., Szidat, S., Wagner, N. L., Weber, R. J., Zotter, P., and Parrish, D. D.: Gasoline emissions dominate over diesel in formation of secondary organic aerosol mass, Geophys. Res. Lett., 39, L06805, doi:10.1029/2011gl050718, 2012.

Title Page

Abstract | Introduction

Conclusions | References

Tables | Figures

|◄ | ►|

◄ | ►

Back | Close

Full Screen / Esc

Printer-friendly Version

Interactive Discussion

Bierbach, A., Barnes, I., and Becker, K. H.: Rate coefficients for the gas-phase reactions of hydroxyl radicals with furan, 2-methylfuran, 2-ethylfuran and 2,5-dimethylfuran at 300+/−2-K, Atmos. Environ., 26, 813–817, 1992.

Bierbach, A., Barnes, I., and Becker, K. H.: Product and kinetic study of the oh-initiated gas-phase oxidation of furan, 2-methylfuran and furanaldehydes at ≈ 300 K, Atmos. Environ., 29, 2651–2660, doi:10.1016/1352-2310(95)00096-H, 1995.

Burling, I. R., Yokelson, R. J., Griffith, D. W. T., Johnson, T. J., Veres, P., Roberts, J. M., Warneke, C., Urbanski, S. P., Reardon, J., Weise, D. R., Hao, W. M., and de Gouw, J.: Laboratory measurements of trace gas emissions from biomass burning of fuel types from the southeastern and southwestern United States, Atmos. Chem. Phys., 10, 11115–11130, doi:10.5194/acp-10-11115-2010, 2010.

Burling, I. R., Yokelson, R. J., Akagi, S. K., Urbanski, S. P., Wold, C. E., Griffith, D. W. T., Johnson, T. J., Reardon, J., and Weise, D. R.: Airborne and ground-based measurements of the trace gases and particles emitted by prescribed fires in the United States, Atmos. Chem. Phys., 11, 12197–12216, doi:10.5194/acp-11-12197-2011, 2011.

Christian, T. J., Kleiss, B., Yokelson, R. J., Holzinger, R., Crutzen, P. J., Hao, W. M., Saharjo, B. H., and Ward, D. E.: Comprehensive laboratory measurements of biomass-burning emissions: 1. Emissions from Indonesian, African, and other fuels, J. Geophys. Res.-Atmos., 108, 4719, doi:10.1029/2003JD003704, 2003.

Christian, T. J., Kleiss, B., Yokelson, R. J., Holzinger, R., Crutzen, P. J., Hao, W. M., Shirai, T., and Blake, D. R.: Comprehensive laboratory measurements of biomass-burning emissions: 2. First intercomparison of open-path FTIR, PTR-MS, and GC- MS/FID/ECD, J. Geophys. Res.-Atmos., 109, D02311, doi:10.1029/2003JD003874, 2004.

Crutzen, P. J. and Andreae, M. O.: Biomass burning in the Tropics – impact on atmospheric chemistry and biogeochemical cycles, Science, 250, 1669–1678, doi:10.1126/science.250.4988.1669, 1990.

de Gouw, J. A., Warneke, C., Parrish, D. D., Holloway, J. S., Trainer, M., and Fehsenfeld, F. C.: Emission sources and ocean uptake of acetonitrile ($CH_3CN$) in the atmosphere, J. Geophys. Res.-Atmos., 108, 4329, doi:10.1029/2002jd002897, 2003.

de Gouw, J. A., Middlebrook, A. M., Warneke, C., Goldan, P. D., Kuster, W. C., Roberts, J. M., Fehsenfeld, F. C., Worsnop, D. R., Canagaratna, M. R., Pszenny, A. A. P., Keene, W. C., Marchewka, M., Bertman, S. B., and Bates, T. S.: Budget of organic carbon in a polluted

Title Page

Abstract | Introduction

Conclusions | References

Tables | Figures

|◄ | ►|

◄ | ►

Back | Close

Full Screen / Esc

Printer-friendly Version

Interactive Discussion

atmosphere: results from the New England Air Quality Study in 2002, J. Geophys. Res.-Atmos., 110, D16305, doi:10.1029/2004JD005623, 2005.

de Gouw, J. A., Warneke, C., Stohl, A., Wollny, A. G., Brock, C. A., Cooper, O. R., Holloway, J. S., Trainer, M., Fehsenfeld, F. C., Atlas, E. L., Donnelly, S. G., Stroud, V., and Lueb, A.: Volatile organic compounds composition of merged and aged forest fire plumes from Alaska and western Canada, J. Geophys. Res.-Atmos., 111, D10303, doi:10.1029/2005JD006175, 2006.

Demirbas, M. F. and Demirbas, T.: Hazardous emissions from combustion of biomass, Energ. Source., 31, 527–534, doi:10.1080/15567030802466953, 2009.

Derwent, R. G., Jenkin, M. E., Utembe, S. R., Shallcross, D. E., Murrells, T. P., and Passant, N. R.: Secondary organic aerosol formation from a large number of reactive man-made organic compounds, Sci. Total Environ., 408, 3374–3381, doi:10.1016/j.scitotenv.2010.04.013, 2010.

Estrellan, C. R. and Iino, F.: Toxic emissions from open burning, Chemosphere, 80, 193–207, doi:10.1016/j.chemosphere.2010.03.057, 2010.

Fischer, E. V., Jacob, D. J., Yantosca, R. M., Sulprizio, M. P., Millet, D. B., Mao, J., Paulot, F., Singh, H. B., Roiger, A., Ries, L., Talbot, R.W., Dzepina, K., and Pandey Deolal, S.: Atmospheric peroxyacetyl nitrate (PAN): a global budget and source attribution, Atmos. Chem. Phys., 14, 2679–2698, doi:10.5194/acp-14-2679-2014, 2014.

Friedli, H. R., Atlas, E., Stroud, V. R., Giovanni, L., Campos, T., and Radke, L. F.: Volatile organic trace gases emitted from North American wildfires, Global Biogeochem. Cy., 15, 435–452, 2001.

Gerbig, C., Schmitgen, S., Kley, D., Volz-Thomas, A., Dewey, K., and Haaks, D.: An improved fast-response vacuum-UV resonance fluorescence CO instrument, J. Geophys. Res.-Atmos., 104, 1699–1704, 1999.

Gilman, J. B., Kuster, W. C., Goldan, P. D., Herndon, S. C., Zahniser, M. S., Tucker, S. C., Brewer, W. A., Lerner, B. M., Williams, E. J., Harley, R. A., Fehsenfeld, F. C., Warneke, C., and de Gouw, J. A.: Measurements of volatile organic compounds during the 2006 TexAQS/GoMACCS campaign: industrial influences, regional characteristics, and diurnal dependencies of the OH reactivity, J. Geophys. Res.-Atmos., 114, D00F06, doi:10.1029/2008jd011525, 2009.

Gilman, J. B., Burkhart, J. F., Lerner, B. M., Williams, E. J., Kuster, W. C., Goldan, P. D., Murphy, P. C., Warneke, C., Fowler, C., Montzka, S. A., Miller, B. R., Miller, L., Oltmans, S. J., Ryerson, T. B., Cooper, O. R., Stohl, A., and de Gouw, J. A.: Ozone variability and halogen

oxidation within the Arctic and sub-Arctic springtime boundary layer, Atmos. Chem. Phys., 10, 10223–10236, doi:10.5194/acp-10-10223-2010, 2010.

Goldan, P. D., Kuster, W. C., Williams, E., Murphy, P. C., Fehsenfeld, F. C., and Meagher, J.: Nonmethane hydrocarbon and oxy hydrocarbon measurements during the 2002 New England Air Quality Study, J. Geophys. Res.-Atmos., 109, D21309, doi:10.1029/2003JD004455, 2004.

Hatch, L. E., Luo, W., Pankow, J. F., Yokelson, R. J., Stockwell, C. E., and Barsanti, K. C.: Identification and quantification of gaseous organic compounds emitted from biomass burning using two-dimensional gas chromatography–time-of-flight mass spectrometry, Atmos. Chem. Phys., 15, 1865–1899, doi:10.5194/acp-15-1865-2015, 2015.

Hegg, D. A., Radke, L. F., Hobbs, P. V., Rasmussen, R. A., and Riggan, P. J.: Emissions of some trace gases from biomass fires, J. Geophys. Res.-Atmos., 95, 5669–5675, doi:10.1029/JD095iD05p05669, 1990.

Heilman, W. E., Liu, Y., Urbanski, S., Kovalev, V., and Mickler, R.: Wildland fire emissions, carbon, and climate: plume rise, atmospheric transport, and chemistry processes, Forest Ecol. Manag., 317, 70–79, doi:10.1016/j.foreco.2013.02.001, 2014.

Holzinger, R., Warneke, C., Hansel, A., Jordan, A., Lindinger, W., Scharffe, D. H., Schade, G., and Crutzen, P. J.: Biomass burning as a source of formaldehyde, acetaldehyde, methanol, acetone, acetonitrile, and hydrogen cyanide, Geophys. Res. Lett., 26, 1161–1164, doi:10.1029/1999gl900156, 1999.

Jaffe, D. A. and Wigder, N. L.: Ozone production from wildfires: a critical review, Atmos. Environ., 51, 1–10, doi:10.1016/j.atmosenv.2011.11.063, 2012.

Karl, T. G., Christian, T. J., Yokelson, R. J., Artaxo, P., Hao, W. M., and Guenther, A.: The Tropical Forest and Fire Emissions Experiment: method evaluation of volatile organic compound emissions measured by PTR-MS, FTIR, and GC from tropical biomass burning, Atmos. Chem. Phys., 7, 5883–5897, doi:10.5194/acp-7-5883-2007, 2007.

Kroll, J. H. and Seinfeld, J. H.: Chemistry of secondary organic aerosol: formation and evolution of low-volatility organics in the atmosphere, Atmos. Environ., 42, 3593–3624, doi:10.1016/j.atmosenv.2008.01.003, 2008.

Manion, J. A., Huie, R. E., Levin, R. D., Burgess Jr., D. R., Orkin, V. L., Tsang, W., McGivern, W. S., Hudgens, J. W., Knyazev, V. D., Atkinson, D. B., Chai, E., Tereza, A. M., Lin, C. J., Allison, T. C., Mallard, W. G., Westley, F., Herron, J. T., Hampson, R. F., and

Title Page

Abstract | Introduction

Conclusions | References

Tables | Figures

|◄ | ►|

◄ | ►

Back | Close

Full Screen / Esc

Printer-friendly Version

Interactive Discussion

Frizzell, D. H.: NIST Standard Reference Database 17, Version 7.0, Web Version available at: http://kinetics.nist.gov/ (last access: 21 February 2015), 2015.

Mason, S. A., Trentmann, J., Winterrath, T., Yokelson, R. J., Christian, T. J., Carlson, L. J., Warner, T. R., Wolfe, L. C., and Andreae, M. O.: Intercomparison of two box models of the chemical evolution in biomass-burning smoke plumes, J. Atmos. Chem., 55, 273–297, doi:10.1007/s10874-006-9039-5, 2006.

McDonald, J. D., Zielinska, B., Fujita, E. M., Sagebiel, J. C., Chow, J. C., and Watson, J. G.: Fine particle and gaseous emission rates from residential wood combustion, Environ. Sci. Technol., 34, 2080–2091, doi:10.1021/es9909632, 2000.

McMeeking, G. R., Kreidenweis, S. M., Baker, S., Carrico, C. M., Chow, J. C., Collett, J. L., Hao, W. M., Holden, A. S., Kirchstetter, T. W., Malm, W. C., Moosmuller, H., Sullivan, A. P., and Wold, C. E.: Emissions of trace gases and aerosols during the open combustion of biomass in the laboratory, J. Geophys. Res.-Atmos., 114, D19210, doi:10.1029/2009jd011836, 2009.

Odum, J. R., Jungkamp, T. P. W., Griffin, R. J., Flagan, R. C., and Seinfeld, J. H.: The atmospheric aerosol-forming potential of whole gasoline vapor, Science, 276, 96–99, 1997.

Pandis, S. N., Harley, R. A., Cass, G. R., and Seinfeld, J. H.: Secondary organic aerosol formation and transport, Atmos. Environ., 26, 2269–2282, 1992.

Pankow, J. F.: An absorption model of the gas-aerosol partitioning involved in the formation of secondary organic aerosol, Atmos. Environ., 28, 189–193, doi:10.1016/1352-2310(94)90094-9, 1994.

Roberts, J. M., Marchewka, M., Bertman, S. B., Sommariva, R., Warneke, C., de Gouw, J., Kuster, W., Goldan, P., Williams, E., Lerner, B. M., Murphy, P., and Fehsenfeld, F. C.: Measurements of PANs during the New England air quality study 2002, J. Geophys. Res.-Atmos., 112, D20306, doi:10.1029/2007JD008667, 2007.

Roberts, J. M., Veres, P., Warneke, C., Neuman, J. A., Washenfelder, R. A., Brown, S. S., Baasandorj, M., Burkholder, J. B., Burling, I. R., Johnson, T. J., Yokelson, R. J., and de Gouw, J.: Measurement of HONO, HNCO, and other inorganic acids by negative-ion proton-transfer chemical-ionization mass spectrometry (NI-PT-CIMS): application to biomass burning emissions, Atmos. Meas. Tech., 3, 981–990, doi:10.5194/amt-3-981-2010, 2010.

Roberts, J. M., Veres, P. R., Cochran, A. K., Warneke, C., Burling, I. R., Yokelson, R. J., Lerner, B., Gilman, J. B., Kuster, W. C., Fall, R., and de Gouw, J.: Isocyanic acid in the atmosphere and its possible link to smoke-related health effects, P. Natl. Acad. Sci. USA, 108, 8966–8971, doi:10.1073/pnas.1103352108, 2011.

Schauer, J. J., Kleeman, M. J., Cass, G. R., and Simoneit, B. R. T.: Measurement of emissions from air pollution sources. 3. C-1-C-29 organic compounds from fireplace combustion of wood, Environ. Sci. Technol., 35, 1716–1728, doi:10.1021/es001331e, 2001.

Simpson, I. J., Akagi, S. K., Barletta, B., Blake, N. J., Choi, Y., Diskin, G. S., Fried, A., Fuelberg, H. E., Meinardi, S., Rowland, F. S., Vay, S. A., Weinheimer, A. J., Wennberg, P. O., Wiebring, P., Wisthaler, A., Yang, M., Yokelson, R. J., and Blake, D. R.: Boreal forest fire emissions in fresh Canadian smoke plumes: $C_1$-$C_{10}$ volatile organic compounds (VOCs), $CO_2$, CO, $NO_2$, NO, HCN and $CH_3CN$, Atmos. Chem. Phys., 11, 6445–6463, doi:10.5194/acp-11-6445-2011, 2011.

Sommers, W. T., Loehman, R. A., and Hardy, C. C.: Wildland fire emissions, carbon, and climate: science overview and knowledge needs, Forest Ecol. Manag., 317, 1–8, doi:10.1016/j.foreco.2013.12.014, 2014.

Stockwell, C. E., Yokelson, R. J., Kreidenweis, S. M., Robinson, A. L., DeMott, P. J., Sullivan, R. C., Reardon, J., Ryan, K. C., Griffith, D. W. T., and Stevens, L.: Trace gas emissions from combustion of peat, crop residue, domestic biofuels, grasses, and other fuels: configuration and Fourier transform infrared (FTIR) component of the fourth Fire Lab at Missoula Experiment (FLAME-4), Atmos. Chem. Phys., 14, 9727–9754, doi:10.5194/acp-14-9727-2014, 2014.

Stockwell, C. E., Veres, P. R., Williams, J., and Yokelson, R. J.: Characterization of biomass burning emissions from cooking fires, peat, crop residue, and other fuels with high-resolution proton-transfer-reaction time-of-flight mass spectrometry, Atmos. Chem. Phys., 15, 845–865, doi:10.5194/acp-15-845-2015, 2015.

Trentmann, J., Andreae, M. O., and Graf, H. F.: Chemical processes in a young biomass-burning plume, J. Geophys. Res.-Atmos., 108, 4705–4714, doi:10.1029/2003jd003732, 2003.

Trentmann, J., Yokelson, R. J., Hobbs, P. V., Winterrath, T., Christian, T. J., Andreae, M. O., and Mason, S. A.: An analysis of the chemical processes in the smoke plume from a savanna fire, J. Geophys. Res.-Atmos., 110, D12301, doi:10.1029/2004jd005628, 2005.

Tuazon, E. C., Alvarado, A., Aschmann, S. M., Atkinson, R., and Arey, J.: Products of the gas-phase reactions of 1,3-butadiene with OH and $NO_3$ Radicals, Environ. Sci. Technol., 33, 3586–3595, doi:10.1021/es990193u, 1999.

Urbanski, S.: Wildland fire emissions, carbon, and climate: emission factors, Forest. Ecol. Manag., 317, 51–60, doi:10.1016/j.foreco.2013.05.045, 2014.

Title Page

Abstract | Introduction

Conclusions | References

Tables | Figures

|◀ | ▶|

◀ | ▶

Back | Close

Full Screen / Esc

Printer-friendly Version

Interactive Discussion

Veres, P., Roberts, J. M., Burling, I. R., Warneke, C., de Gouw, J., and Yokelson, R. J.: Measurements of gas-phase inorganic and organic acids from biomass fires by negative-ion proton-transfer chemical-ionization mass spectrometry, J. Geophys. Res.-Atmos., 115, D23302, doi:10.1029/2010jd014033, 2010.

5 Warneke, C., Roberts, J. M., Veres, P., Gilman, J., Kuster, W. C., Burling, I., Yokelson, R., and de Gouw, J. A.: VOC identification and inter-comparison from laboratory biomass burning using PTR-MS and PIT-MS, Int. J. Mass Spectrom., 303, 6–14, doi:10.1016/j.ijms.2010.12.002, 2011.

Yokelson, R. J., Griffith, D. W. T., and Ward, D. E.: Open-path Fourier transform infrared studies
10 of large-scale laboratory biomass fires, J. Geophys. Res.-Atmos., 101, 21067–21080, 1996.

Yokelson, R. J., Burling, I. R., Gilman, J. B., Warneke, C., Stockwell, C. E., de Gouw, J., Akagi, S. K., Urbanski, S. P., Veres, P., Roberts, J. M., Kuster, W. C., Reardon, J., Griffith, D. W. T., Johnson, T. J., Hosseini, S., Miller, J. W., Cocker III, D. R., Jung, H., and Weise, D. R.: Coupling field and laboratory measurements to estimate the emission factors
15 of identified and unidentified trace gases for prescribed fires, Atmos. Chem. Phys., 13, 89–116, doi:10.5194/acp-13-89-2013, 2013.

**Table 1.** Instrument description.

| Name | Instrument | Meas. Description | Sampling Limitations | References |
|---|---|---|---|---|
| **GC-MS** | *Gas chromatograph-(Quadrupole) Mass Spectrometer* | Discrete sampling via cryogenic pre-concentration, chromatographic separation, and identification via retention time and electron impact ionization mass spectrum | Melting point $> -185\,^\circ$C boiling point $< 220\,^\circ$C sufficiently non-polar mass frag. ($m/z$): 26 to 150 a.m.u | Goldan et al. (2004) Gilman et al. (2010) |
| **PTR-MS** | *Proton Transfer Reaction-(Quadrupole) Mass Spectrometer* | Real-time sampling via proton transfer reactions with $H_3O^+$ and identification via protonated ion $(M+H)^+$ with quadrupole mass filter | Proton affinity greater than water; Protonated molecular mass or mass fragment ($m/z$): 20–240 a.m.u | Warneke et al. (2011) |
| **PIT-MS** | *Proton Transfer Reaction-(Ion Trap) Mass Spectrometer* | Real-time sampling via proton transfer reactions with $H_3O^+$ and identification via protonated ion $(M+H)^+$ with ion trap mass spectrometer | Proton affinity greater than water; Protonated molecular mass or mass fragment ($m/z$): 20–240 a.m.u | Warneke et al. (2011) |
| **NI-PT-CIMS** | *Negative Ion-Proton Transfer Reaction-(Quadrupole) Mass Spectrometer* | Real-time sampling via proton transfer reactions with $CH_3C(O)O^-$ and identification via deprotonated ion $(M-H)^-$ with quadrupole mass filter | Gas-phase acidity greater than that of acetic acid; Deprotonated molecular mass or mass fragment ($m/z$): 10–225 a.m.u | Veres et al. (2011) Roberts et al. (2011) |
| **OP-FTIR** | *Open Path-Fourier Transform Infrared Spectrometer* | Real-time spectral scanning via open path White cell, offline identification via compound specific infrared absorption features | Strong absoprtion features between 600–3400 cm$^{-1}$ that are unique and have minimal interferences from other strong infrared-absorbers | Burling et al. (2011) |

ACPD

15, 21713–21763, 2015

Biomass burning emissions and potential air quality impacts

J. B. Gilman et al.

Title Page

Abstract | Introduction

Conclusions | References

Tables | Figures

|◀ | ▶|

◀ | ▶

Back | Close

Full Screen / Esc

Printer-friendly Version

Interactive Discussion

**Table 2.** Mean VOC to CO discrete emission ratios (ERs) for the southwestern (SW), southeastern (SE), and northern (N) fuel regions.

| Name | Formula | MW | $D$ | $m/z$ | SW Avg | (±SD) | npnts | SE Avg | (±SD) | npnts | N Avg | (±SD) | npnts |
|---|---|---|---|---|---|---|---|---|---|---|---|---|---|
| **Alkanes (Saturated, $D$ = 0)** | | | | | | | | | | | | | |
| Ethane | C2H6 | 30 | 0 | 27 | **1.8388** | (1.2846) | 25 | **4.5311** | (3.8024) | 23 | **6.8510** | (3.5152) | 4 |
| Propane | C3H8 | 44 | 0 | 27 | **0.6317** | (0.9985) | 23 | **1.5957** | (1.2193) | 18 | **1.4633** | (0.9354) | 4 |
| Butane_iso | C4H10 | 58 | 0 | 43 | 0.0522 | (0.0813) | 29 | 0.2984 | (0.4734) | 20 | 0.0982 | (0.0620) | 4 |
| Butane_n | C4H10 | 58 | 0 | 43 | **0.1038** | (0.1829) | 29 | **0.3333** | (0.2902) | 20 | **0.4005** | (0.2804) | 4 |
| Propane_22dimethyl | C5H12 | 72 | 0 | 57 | 0.0003 | (0.0008) | 29 | 0.0004 | (0.0008) | 23 | 0.0006 | (0.0007) | 4 |
| Pentane_iso | C5H12 | 72 | 0 | 43 | 0.0167 | (0.0585) | 29 | 0.0580 | (0.0878) | 23 | 0.0322 | (0.0261) | 4 |
| Pentane_n | C5H12 | 72 | 0 | 43 | 0.0271 | (0.0427) | 29 | 0.0889 | (0.0789) | 23 | 0.1400 | (0.1130) | 4 |
| Butane_22dimethyl | C6H14 | 86 | 0 | 71 | 0.0002 | (0.0008) | 29 | 0.0001 | (0.0002) | 23 | | | 0 |
| Pentane_3methyl | C6H14 | 86 | 0 | 57 | 0.0009 | (0.0010) | 9 | 0.0089 | (0.0117) | 16 | 0.0045 | (0.0031) | 4 |
| Hexane_n | C6H14 | 86 | 0 | 57 | 0.0159 | (0.0225) | 29 | 0.0572 | (0.0516) | 23 | 0.0814 | (0.0634) | 4 |
| Heptane_n | C7H16 | 100 | 0 | 43 | 0.0218 | (0.0176) | 9 | 0.0640 | (0.0387) | 14 | 0.0836 | (0.0674) | 4 |
| Octane_n | C8H18 | 114 | 0 | 43 | 0.0138 | (0.0128) | 9 | 0.0469 | (0.0281) | 14 | 0.0536 | (0.0353) | 4 |
| Nonane_n | C9H20 | 128 | 0 | 57 | 0.0085 | (0.0079) | 9 | 0.0358 | (0.0213) | 13 | 0.0369 | (0.0269) | 4 |
| Decane_n | C10H22 | 142 | 0 | 57 | 0.0083 | (0.0060) | 9 | 0.0310 | (0.0222) | 14 | 0.0330 | (0.0212) | 4 |
| Undecane_n | C11H24 | 156 | 0 | 57 | 0.0111 | (0.0054) | 8 | 0.0412 | (0.0304) | 12 | 0.0425 | (0.0208) | 4 |
| | | | | | | | | | | | | | |
| **Alkenes (Saturated, $D$ = 1)** | | | | | | | | | | | | | |
| Ethene | C2H4 | 28 | 1 | 27 | **5.8525** | (4.1077) | 25 | **8.1879** | (4.2382) | 21 | **18.3160** | (12.8430) | 4 |
| Propene | C3H6 | 42 | 1 | 41 | **2.0801** | (2.0528) | 29 | **3.4917** | (2.1610) | 23 | **8.5115** | (3.4340) | 4 |
| Propene_2methyl | C4H8 | 56 | 1 | 41 | 0.1046 | (0.1652) | 29 | 0.2668 | (0.2151) | 23 | 0.3162 | (0.3624) | 4 |
| Butene_1 | C4H8 | 56 | 1 | 41 | **0.2961** | (0.3761) | 29 | **0.4851** | (0.3320) | 23 | **1.5227** | (0.6632) | 4 |
| Butene_cis2 | C4H8 | 56 | 1 | 41 | 0.0579 | (0.0937) | 29 | 0.1209 | (0.0920) | 23 | 0.2397 | (0.1916) | 4 |
| Butene_trans2 | C4H8 | 56 | 1 | 41 | 0.0615 | (0.1036) | 29 | 0.1427 | (0.1174) | 23 | 0.2732 | (0.2648) | 4 |
| Butene_1_2methyl | C5H10 | 70 | 1 | 55 | 0.0202 | (0.0256) | 29 | 0.0391 | (0.0284) | 23 | 0.0881 | (0.0462) | 4 |
| Butene_1_3methyl | C5H10 | 70 | 1 | 55 | 0.0091 | (0.0202) | 8 | 0.0152 | (0.0168) | 15 | 0.0183 | (0.0164) | 4 |
| Butene_2_2methyl | C5H10 | 70 | 1 | 55 | 0.0224 | (0.0317) | 29 | 0.0996 | (0.0634) | 14 | 0.1881 | (0.0965) | 4 |
| Cyclopentane | C5H10 | 70 | 1 | 42 | 0.0024 | (0.0040) | 29 | 0.0064 | (0.0053) | 23 | 0.0108 | (0.0074) | 4 |
| Pentene_1 | C5H10 | 70 | 1 | 55 | 0.0429 | (0.0654) | 29 | 0.0902 | (0.0773) | 23 | 0.2311 | (0.1872) | 4 |
| Pentene_cis2 | C5H10 | 70 | 1 | 55 | 0.0432 | (0.0638) | 8 | 0.1396 | (0.0883) | 14 | 0.2905 | (0.1492) | 4 |
| Pentene_trans2 | C5H10 | 70 | 1 | 55 | 0.0276 | (0.0341) | 29 | 0.0422 | (0.0304) | 23 | 0.1180 | (0.0667) | 4 |
| Cyclopentane_1methyl | C6H12 | 84 | 1 | 56 | 0.0040 | (0.0037) | 9 | 0.0147 | (0.0139) | 16 | 0.0159 | (0.0113) | 4 |
| Pentene_1_2methyl | C6H12 | 84 | 1 | 56 | 0.0890 | (0.1102) | 9 | 0.1782 | (0.1162) | 14 | 0.4980 | (0.2945) | 4 |
| Cyclohexane | C6H12 | 84 | 1 | 84 | 0.0012 | (0.0014) | 9 | 0.0052 | (0.0028) | 14 | 0.0052 | (0.0035) | 4 |
| Hexene_1 | C6H12 | 84 | 1 | 84 | 0.1029 | (0.1182) | 8 | 0.2039 | (0.0943) | 12 | 0.4904 | (0.2844) | 4 |
| Hexene_cis2 | C6H12 | 84 | 1 | 84 | 0.0256 | (0.0338) | 9 | 0.0522 | (0.0443) | 16 | 0.1552 | (0.0586) | 4 |
| Hexenes (sum of 3 isomers) | C6H12 | 84 | 1 | 84 | 0.0931 | (0.1166) | 9 | 0.1788 | (0.1376) | 16 | 0.5432 | (0.2920) | 4 |
| Cyclohexane_methyl | C7H14 | 98 | 1 | 83 | 0.0023 | (0.0023) | 8 | 0.0097 | (0.0063) | 14 | 0.0111 | (0.0071) | 4 |
| Heptene_1 | C7H14 | 98 | 1 | 56 | 0.0547 | (0.0595) | 9 | 0.1168 | (0.0721) | 14 | 0.2868 | (0.1559) | 4 |
| Octene_1 | C8H16 | 112 | 1 | 55 | 0.0431 | (0.0486) | 9 | 0.1013 | (0.0482) | 13 | 0.1651 | (0.0926) | 4 |
| Nonene_1 | C9H18 | 126 | 1 | 41 | 0.0097 | (0.0122) | 9 | 0.0196 | (0.0153) | 16 | 0.0474 | (0.0326) | 4 |
| Decene_1 | C10H20 | 140 | 1 | 56 | 0.0133 | (0.0159) | 9 | 0.0260 | (0.0228) | 16 | 0.0812 | (0.0415) | 4 |
| Undecene_1 | C11H22 | 154 | 1 | 55 | 0.0103 | (0.0100) | 9 | 0.0279 | (0.0292) | 16 | 0.0647 | (0.0251) | 4 |

**Table 2.** Continued.

| Name | Formula | MW | D | m/z | SW Avg | (±SD) | npnts | SE Avg | (±SD) | npnts | N Avg | (±SD) | npnts |
|---|---|---|---|---|---|---|---|---|---|---|---|---|---|
| **Alkynes and Alkenes (Polyunsaturated, $D > 0$)** | | | | | | | | | | | | | |
| Ethyne | C2H2 | 26 | 2 | IR | **2.3905** | (3.0119) | 27 | **1.7412** | (1.3580) | 23 | **5.0910** | (5.6894) | 4 |
| Propyne | C3H4 | 40 | 2 | 39 | **0.2093** | (0.1503) | 29 | **0.1850** | (0.1626) | 23 | **0.7876** | (0.6405) | 4 |
| Butadiyne_13 (Diacetylene) | C4H2 | 50 | 4 | 50 | 0.0080 | (0.0054) | 9 | 0.0041 | (0.0052) | 16 | 0.0427 | (0.0651) | 4 |
| Butenyne (Vinylacetylene) | C4H4 | 52 | 3 | 52 | 0.0285 | (0.0452) | 9 | 0.0154 | (0.0190) | 16 | 0.0824 | (0.1062) | 4 |
| Butadiene_12 | C4H6 | 54 | 2 | 54 | 0.0101 | (0.0146) | 29 | 0.0087 | (0.0095) | 23 | 0.0441 | (0.0343) | 4 |
| Butadiene_13 | C4H6 | 54 | 2 | 54 | **0.4065** | (0.5315) | 29 | **0.4122** | (0.3530) | 23 | **1.8781** | (0.9509) | 4 |
| Butyne (1- or 2-) | C4H6 | 54 | 2 | 54 | 0.0221 | (0.0287) | 9 | 0.0158 | (0.0146) | 16 | 0.0693 | (0.0300) | 4 |
| Cyclopentadiene_13 | C5H6 | 66 | 3 | 66 | 0.1724 | (0.3868) | 8 | 0.1747 | (0.0992) | 14 | 0.5836 | (0.3458) | 4 |
| Pentenyne isomer (e.g., propenylacetylene) | C5H6 | 66 | 3 | 66 | 0.0161 | (0.0176) | 9 | 0.0107 | (0.0119) | 16 | 0.0651 | (0.0395) | 4 |
| Butyne_3methyl | C5H8 | 68 | 2 | 67 | 0.0090 | (0.0166) | 9 | 0.0103 | (0.0108) | 16 | 0.0426 | (0.0303) | 4 |
| Cyclopentene | C5H8 | 68 | 2 | 67 | 0.0699 | (0.1240) | 7 | 0.1125 | (0.0789) | 14 | 0.2815 | (0.1725) | 4 |
| Pentadiene_cis13 | C5H8 | 68 | 2 | 67 | 0.0457 | (0.0795) | 8 | 0.0627 | (0.0360) | 14 | 0.1733 | (0.0691) | 4 |
| Pentadiene_trans13 | C5H8 | 68 | 2 | 67 | 0.0668 | (0.1069) | 9 | 0.1044 | (0.0538) | 14 | 0.2504 | (0.0927) | 4 |
| Hexadienyne (e.g., divinylacetylene) | C6H6 | 78 | 4 | 78 | 0.0140 | (0.0152) | 9 | 0.0088 | (0.0072) | 16 | 0.0569 | (0.0382) | 4 |
| Cyclopentadiene_methyl (sum of 2 isomers) | C6H8 | 80 | 3 | 79 | 0.0242 | (0.0329) | 9 | 0.0516 | (0.0554) | 9 | 0.1831 | (0.1771) | 4 |
| Hexenyne (e.g., 2-methyl- 1-penten-3-yne) | C6H8 | 80 | 3 | 80 | 0.0110 | (0.0127) | 9 | 0.0102 | (0.0117) | 16 | 0.0674 | (0.0545) | 4 |
| Cyclohexene | C6H10 | 82 | 2 | 67 | 0.0170 | (0.0235) | 9 | 0.0345 | (0.0205) | 14 | 0.0927 | (0.0506) | 4 |
| Cyclopentene_1methyl | C6H10 | 82 | 2 | 67 | 0.0202 | (0.0298) | 9 | 0.0466 | (0.0259) | 13 | 0.1109 | (0.0539) | 4 |
| Hexadiene_cis13 | C6H10 | 82 | 2 | 67 | 0.0026 | (0.0037) | 9 | 0.0044 | (0.0030) | 14 | 0.0097 | (0.0018) | 4 |
| Hexadiene_trans13 | C6H10 | 82 | 2 | 67 | 0.0039 | (0.0081) | 9 | 0.0045 | (0.0042) | 12 | 0.0266 | (0.0151) | 4 |
| Other C6H10 (sum of 5 isomers) | C6H10 | 82 | 2 | 67 | 0.0348 | (0.0466) | 9 | 0.0531 | (0.0418) | 16 | 0.1954 | (0.0798) | 4 |
| Heptadiyne (sum of 2 isomers) | C7H8 | 92 | 4 | 91 | 0.0073 | (0.0094) | 9 | 0.0035 | (0.0053) | 16 | 0.0464 | (0.0394) | 4 |
| Cyclohexene_1methyl | C7H12 | 96 | 2 | 81 | 0.0098 | (0.0120) | 8 | 0.0262 | (0.0139) | 13 | 0.0437 | (0.0259) | 4 |
| Octadiene | C8H14 | 110 | 2 | 55 | 0.0347 | (0.0531) | 9 | 0.0673 | (0.0416) | 16 | 0.1387 | (0.0536) | 4 |
| Nonadiene | C9H16 | 124 | 2 | 54 | 0.0020 | (0.0027) | 9 | 0.0048 | (0.0048) | 16 | 0.0171 | (0.0077) | 4 |
| C10H14 non-aromatic (e.g., hexahydronaphthalene) | C10H14 | 134 | 4 | 91 | 0.0013 | (0.0018) | 9 | 0.0041 | (0.0055) | 16 | 0.0155 | (0.0090) | 4 |
| | | | | | | | | | | | | | |
| **Terpenes (Polyunsaturated $D > 1$)** | | | | | | | | | | | | | |
| Isoprene | C5H8 | 68 | 2 | 67 | **0.1289** | (0.1447) | 29 | **0.2428** | (0.1944) | 23 | **0.6942** | (0.4405) | 4 |
| Camphene | C10H16 | 136 | 3 | 93 | 0.0032 | (0.0026) | 9 | 0.0538 | (0.0979) | 14 | 0.1193 | (0.1459) | 4 |
| Carene_3 | C10H16 | 136 | 3 | 93 | 0.0050 | (0.0052) | 8 | 0.0289 | (0.0303) | 12 | 0.1578 | (0.2107) | 4 |
| Limonene_D | C10H16 | 136 | 3 | 68 | **0.0219** | (0.0249) | 29 | **0.1232** | (0.1302) | 23 | **0.8384** | (1.1869) | 4 |
| Limonene_iso | C10H16 | 136 | 3 | 68 | 0.0002 | (0.0005) | 9 | 0.0094 | (0.0109) | 16 | 0.0237 | (0.0206) | 4 |
| Myrcene | C10H16 | 136 | 3 | 93 | 0.0075 | (0.0106) | 8 | 0.0068 | (0.0055) | 10 | 0.1313 | (0.1849) | 4 |
| Pinene_alpha | C10H16 | 136 | 3 | 93 | 0.0058 | (0.0051) | 9 | **0.1013** | (0.1454) | 15 | **0.8105** | (1.2079) | 4 |
| Pinene_beta | C10H16 | 136 | 3 | 93 | 0.0051 | (0.0092) | 29 | 0.0194 | (0.0220) | 23 | 0.1638 | (0.1545) | 4 |
| Terpinene_gamma | C10H16 | 136 | 3 | 93 | 0.0044 | (0.0026) | 5 | 0.0118 | (0.0066) | 4 | 0.0310 | (0.0336) | 2 |
| Terpinolene | C10H16 | 136 | 3 | 93 | 0.0053 | (0.0020) | 4 | 0.0131 | (0.0163) | 8 | 0.0339 | (0.0435) | 4 |
| Sesquiterpenes (sum of all isomers) | C15H24 | 204 | 4 | 205+ | **0.0092** | (0.0088) | 29 | 0.0669 | (0.0786) | 23 | 0.0915 | (0.0659) | 4 |

**Table 2.** Continued.

| Name | Formula | MW | $D$ | $m/z$ | SW Avg | (±SD) | npnts | SE Avg | (±SD) | npnts | N Avg | (±SD) | npnts |
|---|---|---|---|---|---|---|---|---|---|---|---|---|---|
| **Aromatics with saturated subsituents ($D = 4$)** | | | | | | | | | | | | | |
| Benzene | C6H6 | 78 | 4 | 78 | **0.8385** | (0.7301) | 29 | **0.7008** | (0.3680) | 23 | **2.1381** | (1.3236) | 4 |
| Toluene | C7H8 | 92 | 4 | 91 | **0.3549** | (0.3417) | 29 | **0.6196** | (0.4414) | 23 | **1.3375** | (0.5725) | 4 |
| Benzene_ethyl | C8H10 | 106 | 4 | 91 | 0.0495 | (0.0498) | 29 | 0.0829 | (0.0583) | 23 | 0.1766 | (0.0919) | 4 |
| Xylene_o | C8H10 | 106 | 4 | 91 | 0.0391 | (0.0418) | 29 | 0.0730 | (0.0527) | 23 | 0.1429 | (0.0579) | 4 |
| Xylenes_m&p (sum of 2 isomers) | C8H10 | 106 | 4 | 91 | 0.0981 | (0.1136) | 29 | **0.2107** | (0.1546) | 23 | **0.5088** | (0.2484) | 4 |
| Benzene_123trimethyl | C9H12 | 120 | 4 | 105 | 0.0150 | (0.0137) | 9 | 0.0617 | (0.0425) | 15 | 0.0906 | (0.0562) | 4 |
| Benzene_124trimethyl | C9H12 | 120 | 4 | 105 | 0.0172 | (0.0217) | 29 | 0.0416 | (0.0291) | 23 | 0.0828 | (0.0339) | 4 |
| Benzene_135trimethyl | C9H12 | 120 | 4 | 105 | 0.0090 | (0.0083) | 9 | 0.0234 | (0.0154) | 15 | 0.0401 | (0.0158) | 4 |
| Benzene_1ethyl_2methyl | C9H12 | 120 | 4 | 105 | 0.0094 | (0.0114) | 9 | 0.0164 | (0.0122) | 15 | 0.0374 | (0.0193) | 4 |
| Benzene_1ethyl_3&4_methyl (sum of 2 isomers) | C9H12 | 120 | 4 | 105 | 0.0186 | (0.0228) | 29 | 0.0395 | (0.0312) | 23 | 0.1265 | (0.0737) | 4 |
| Benzene_isoPropyl | C9H12 | 120 | 4 | 105 | 0.0041 | (0.0042) | 9 | 0.0073 | (0.0065) | 14 | 0.0290 | (0.0211) | 4 |
| Benzene_nPropyl | C9H12 | 120 | 4 | 91 | 0.0081 | (0.0096) | 9 | 0.0173 | (0.0102) | 14 | 0.0331 | (0.0204) | 4 |
| Benzene_isoButyl | C10H14 | 134 | 4 | 91 | 0.0056 | (0.0065) | 9 | 0.0119 | (0.0104) | 16 | 0.0248 | (0.0145) | 4 |
| Benzene_nButyl | C10H14 | 134 | 4 | 91 | 0.0065 | (0.0078) | 9 | 0.0151 | (0.0129) | 16 | 0.0329 | (0.0193) | 4 |
| Benzene_1methyl_4isopropyl (p-Cymene) | C10H14 | 134 | 4 | 119 | **0.1081** | (0.2713) | 29 | 0.1030 | (0.0974) | 23 | 0.1726 | (0.1400) | 4 |
| Benzene_nPropyl_methyl (sum of 2 isomers) | C10H14 | 134 | 4 | 105 | 0.0074 | (0.0084) | 9 | 0.0200 | (0.0187) | 16 | 0.0420 | (0.0213) | 4 |
| Benzene_14diethyl | C10H14 | 134 | 4 | 119 | 0.0007 | (0.0011) | 9 | 0.0018 | (0.0039) | 16 | 0.0165 | (0.0074) | 4 |
| Xylene_ethyl (sum of 2 isomers) | C10H14 | 134 | 4 | 119 | 0.0093 | (0.0102) | 9 | 0.0149 | (0.0144) | 16 | 0.0379 | (0.0158) | 4 |
| | | | | | | | | | | | | | |
| **Aromatics with unsaturated substituents ($D > 4$)** | | | | | | | | | | | | | |
| Benzene_ethynyl (Phenylethyne) | C8H6 | 102 | 6 | 102 | **0.0323** | (0.0238) | 9 | 0.0153 | (0.0163) | 16 | 0.0686 | (0.0700) | 4 |
| Styrene (Phenylethene) | C8H8 | 104 | 5 | 104 | **0.0883** | (0.0840) | 29 | **0.1067** | (0.1054) | 23 | **0.3361** | (0.2437) | 4 |
| Indene | C9H8 | 116 | 6 | 115 | **0.0358** | (0.0446) | 9 | **0.0408** | (0.0325) | 16 | **0.1311** | (0.1116) | 4 |
| Benzene_1propenyl | C9H10 | 118 | 5 | 117 | 0.0046 | (0.0054) | 9 | 0.0039 | (0.0045) | 16 | 0.0135 | (0.0074) | 4 |
| Benzene_2propenyl | C9H10 | 118 | 5 | 117 | 0.0067 | (0.0066) | 9 | 0.0097 | (0.0080) | 16 | 0.0236 | (0.0103) | 4 |
| Benzene_isoPropenyl | C9H10 | 118 | 5 | 118 | 0.0052 | (0.0059) | 9 | 0.0049 | (0.0050) | 16 | 0.0232 | (0.0129) | 4 |
| Styrene_2methyl | C9H10 | 118 | 5 | 117 | 0.0142 | (0.0125) | 9 | 0.0153 | (0.0140) | 16 | 0.0414 | (0.0176) | 4 |
| Styrene_3methyl | C9H10 | 118 | 5 | 117 | 0.0229 | (0.0255) | 9 | **0.0297** | (0.0234) | 16 | **0.0865** | (0.0420) | 4 |
| Styrene_4methyl | C9H10 | 118 | 5 | 117 | 0.0080 | (0.0097) | 9 | 0.0143 | (0.0116) | 16 | 0.0314 | (0.0122) | 4 |
| Indane | C9H10 | 118 | 5 | 117 | 0.0084 | (0.0066) | 8 | 0.0155 | (0.0069) | 13 | 0.0261 | (0.0108) | 4 |
| Naphthalene | C10H8 | 128 | 7 | 128 | 0.0070 | (0.0048) | 9 | 0.0040 | (0.0050) | 16 | 0.0215 | (0.0122) | 4 |
| Indene_1or3methyl | C10H10 | 130 | 6 | 130 | 0.0010 | (0.0009) | 9 | 0.0004 | (0.0011) | 16 | 0.0079 | (0.0059) | 4 |
| Naphthalene_12dihydro | C10H10 | 130 | 6 | 130 | 0.0062 | (0.0054) | 9 | 0.0099 | (0.0103) | 16 | 0.0277 | (0.0106) | 4 |
| Naphthalene_13dihydro | C10H10 | 130 | 6 | 130 | 0.0062 | (0.0066) | 9 | 0.0099 | (0.0113) | 16 | 0.0339 | (0.0120) | 4 |
| Benzene_1butenyl | C10H12 | 132 | 5 | 117 | 0.0021 | (0.0028) | 9 | 0.0027 | (0.0038) | 16 | 0.0140 | (0.0048) | 4 |
| Benzene_methylpropenyl (2-phenyl-2-butene) | C10H12 | 132 | 5 | 117 | 0.0274 | (0.0443) | 9 | 0.0179 | (0.0179) | 16 | 0.0436 | (0.0270) | 4 |
| Styrene_ethyl | C10H12 | 132 | 5 | 117 | 0.0048 | (0.0052) | 9 | 0.0063 | (0.0105) | 16 | 0.0196 | (0.0085) | 4 |

**Table 2.** Continued.

| Name | Formula | MW | D | m/z | SW Avg | (±SD) | npnts | SE Avg | (±SD) | npnts | N Avg | (±SD) | npnts |
|---|---|---|---|---|---|---|---|---|---|---|---|---|---|
| **Nitrogen-containing organics** | | | | | | | | | | | | | |
| Acid_Hydrocyanic (Hydrogen cyanide) | HCN | 27 | 2 | IR | **1.2331** | (1.2922) | 29 | **2.7807** | (1.6904) | 23 | **3.0223** | (2.2719) | 4 |
| Acid_Isocyanic | HNCO | 43 | 2 | 42– | **0.8433** | (0.6858) | 16 | **0.8046** | (0.5742) | 17 | **1.3360** | (0.2301) | 2 |
| Methylnitrite (Nitrous acid, methyl ester) | CH3NO2 | 61 | 1 | 61 | **0.8994** | (1.1114) | 7 | 0.5241 | (0.5064) | 12 | 0.7641 | (0.8964) | 3 |
| Nitromethane | CH3NO2 | 61 | 1 | 61 | 0.0272 | (0.0237) | 9 | 0.0323 | (0.0326) | 16 | 0.0713 | (0.0868) | 4 |
| Acetonitrile | C2H3N | 41 | 2 | 41 | 0.7731 | (0.9389) | 29 | **0.9841** | (0.5366) | 23 | **1.6524** | (0.8811) | 4 |
| Hydrazine_11dimethyl | C2H8N2 | 60 | 0 | 60 | 0.0636 | (0.1324) | 9 | 0.1360 | (0.2705) | 16 | 0.1976 | (0.2297) | 4 |
| Propenenitrile_2 (Acrylonitrile) | C3H3N | 53 | 3 | 53 | 0.0869 | (0.0731) | 29 | 0.1199 | (0.0754) | 23 | 0.3217 | (0.2551) | 4 |
| Propanenitrile (Cyanoethane) | C3H5N | 55 | 2 | 54 | 0.0314 | (0.0380) | 9 | 0.0432 | (0.0366) | 16 | 0.0981 | (0.0803) | 4 |
| Pyrrole | C4H5N | 67 | 3 | 67 | 0.0393 | (0.0591) | 9 | 0.0367 | (0.0392) | 16 | 0.1066 | (0.1088) | 4 |
| Pyrazole_1methyl | C4H6N2 | 82 | 3 | 82 | 0.0074 | (0.0073) | 9 | 0.0198 | (0.0176) | 16 | 0.0359 | (0.0161) | 4 |
| Diazine_methyl (sum of 3 isomers) | C5H6N2 | 94 | 4 | 94 | 0.0292 | (0.0312) | 9 | 0.0535 | (0.0456) | 16 | 0.1125 | (0.0303) | 4 |
| Pyrrole_1methyl | C5H7N | 81 | 3 | 80 | 0.0202 | (0.0299) | 9 | 0.0083 | (0.0105) | 16 | 0.0217 | (0.0304) | 4 |
| Pyrazine_2ethyl | C6H8N2 | 108 | 4 | 108 | 0.0062 | (0.0092) | 9 | 0.0152 | (0.0113) | 16 | 0.0296 | (0.0168) | 4 |
| Benzonitrile (Cyanobenzene) | C7H5N | 103 | 6 | 103 | 0.0622 | (0.0334) | 9 | 0.1395 | (0.0757) | 16 | 0.1380 | (0.0746) | 4 |
| **OVOCs with low degrees of unsaturation (D = 1)** | CH2O | 30 | 1 | IR | | | | | | | | | |
| Formaldehyde | CH2O | 30 | 1 | IR | *5.3939* | (3.1497) | 29 | *12.2348* | (7.2935) | 23 | *17.9180* | (10.5410) | 4 |
| Acid_Formic | CH2O2 | 46 | 1 | IR | 0.6359 | (0.5705) | 29 | 1.6007 | (1.1054) | 23 | 1.7538 | (1.9738) | 4 |
| Methanol | CH4O | 32 | 0 | 31 | **3.6175** | (2.9726) | 29 | **7.7807** | (5.5412) | 23 | **13.6981** | (8.7348) | 4 |
| Acetaldehyde | C2H4O | 44 | 1 | 44 | 1.5503 | (1.1511) | 29 | 2.8332 | (1.8131) | 23 | 5.4742 | (3.5540) | 4 |
| Acid_Acetic | C2H4O2 | 60 | 1 | IR | *5.3926* | (3.2343) | 29 | *13.0293* | (8.8369) | 23 | 9.6068 | (6.2350) | 4 |
| Formate_methyl (Formic Acid, methyl ester) | C2H4O2 | 60 | 1 | 60 | 0.0675 | (0.0390) | 8 | 0.1031 | (0.0626) | 15 | 0.2096 | (0.0831) | 4 |
| Acid_Glycolic | C2H4O3 | 76 | 1 | 75– | 0.0068 | (0.0061) | 15 | 0.1183 | (0.1251) | 17 | 0.0114 | (0.0115) | 2 |
| Ethanol | C2H6O | 46 | 0 | 31 | 0.0498 | (0.0617) | 29 | 0.4817 | (0.8472) | 23 | 0.2673 | (0.1892) | 4 |
| Acetone | C3H6O | 58 | 1 | 43 | 0.6501 | (0.7408) | 29 | 1.6035 | (1.1498) | 23 | 2.6208 | (1.0656) | 4 |
| Propanal | C3H6O | 58 | 1 | 58 | 0.2135 | (0.2333) | 29 | 0.4497 | (0.3177) | 23 | 0.9246 | (0.3186) | 4 |
| Acetate_methyl (Acetic Acid, methyl ester) | C3H6O2 | 74 | 1 | 74 | 0.4593 | (0.4854) | 9 | 0.6741 | (0.4345) | 16 | 0.6537 | (0.3598) | 4 |
| Formate_ethyl (Formic Acid, ethyl ester) | C3H6O2 | 74 | 1 | 30 | 0.0214 | (0.0157) | 5 | 0.0349 | (0.0160) | 10 | 0.0472 | (0.0228) | 4 |
| Butanal_n | C4H8O | 72 | 1 | 72 | 0.0496 | (0.0610) | 29 | 0.0850 | (0.0641) | 23 | 0.1971 | (0.0829) | 4 |
| Butanone_2 (MEK) | C4H8O | 72 | 1 | 43 | 0.1788 | (0.2216) | 29 | 0.4143 | (0.3061) | 23 | 0.8027 | (0.3109) | 4 |
| Propanal_2methyl | C4H8O | 72 | 1 | 72 | 0.0535 | (0.0599) | 9 | 0.1426 | (0.0933) | 15 | 0.1657 | (0.0976) | 4 |
| Propanoate_methyl (Prop- anoic Acid, methyl ester) | C4H8O2 | 88 | 1 | 88 | 0.0064 | (0.0085) | 9 | 0.0081 | (0.0082) | 16 | 0.0186 | (0.0110) | 4 |
| Butanol_1 | C4H10O | 74 | 0 | 56 | 0.8294 | (1.6678) | 8 | 0.2327 | (0.2540) | 16 | 0.1434 | (0.0695) | 4 |
| Butanal_2methyl | C5H10O | 86 | 1 | 57 | 0.0442 | (0.0476) | 9 | 0.1398 | (0.0760) | 13 | 0.1323 | (0.0939) | 4 |
| Butanone_2_3methyl | C5H10O | 86 | 1 | 43 | 0.0243 | (0.0315) | 9 | 0.0780 | (0.0394) | 14 | 0.1092 | (0.0551) | 4 |
| Pentanone_2 | C5H10O | 86 | 1 | 43 | 0.0576 | (0.0457) | 8 | 0.1095 | (0.0537) | 14 | 0.1791 | (0.0935) | 4 |
| Pentanone_3 | C5H10O | 86 | 1 | 57 | 0.0381 | (0.0366) | 8 | 0.0869 | (0.0483) | 15 | 0.1330 | (0.0562) | 4 |
| Butanoate_methyl (Butyric Acid, methyl ester) | C5H10O2 | 102 | 1 | 74 | 0.0024 | (0.0041) | 9 | 0.0558 | (0.1431) | 16 | 0.0097 | (0.0063) | 4 |
| Hexanal_n | C6H12O | 100 | 1 | 56 | 0.0192 | (0.0223) | 29 | 0.0342 | (0.0224) | 23 | 0.0635 | (0.0431) | 4 |
| Hexanone_2 | C6H12O | 100 | 1 | 43 | 0.0101 | (0.0063) | 8 | 0.0269 | (0.0092) | 12 | 0.0462 | (0.0268) | 4 |
| Hexanone_3 | C6H12O | 100 | 1 | 43 | 0.0314 | (0.0315) | 9 | 0.0834 | (0.0317) | 13 | 0.1646 | (0.0868) | 4 |

**Table 2.** Continued.

| Name | Formula | MW | D | m/z | SW Avg | (±SD) | npnts | SE Avg | (±SD) | npnts | N Avg | (±SD) | npnts |
|---|---|---|---|---|---|---|---|---|---|---|---|---|---|
| **OVOCs with high degrees of unsaturation ($D > 1$)** | | | | | | | | | | | | | |
| Propenal_2 (Acrolein) | C3H4O | 56 | 2 | 56 | **0.8189** | (0.6824) | 29 | **1.3107** | (0.8806) | 23 | **3.5441** | (1.6919) | 4 |
| Acid_Acrylic | C3H4O2 | 72 | 2 | 71– | 0.0409 | (0.0438) | 16 | 0.2159 | (0.1637) | 17 | 0.3672 | (0.3881) | 2 |
| Acid_Pyruvic | C3H4O3 | 88 | 2 | 87– | 0.0140 | (0.0140) | 15 | 0.1073 | (0.1266) | 17 | 0.0562 | (0.0537) | 2 |
| Butenal_2 (Crotonaldehyde) | C4H6O | 70 | 2 | 70 | 0.1218 | (0.1286) | 29 | 0.3234 | (0.2207) | 23 | 0.5275 | (0.1642) | 4 |
| Methacrolein (MACR) | C4H6O | 70 | 2 | 41 | 0.0895 | (0.1077) | 29 | 0.1807 | (0.1257) | 23 | 0.5501 | (0.3146) | 4 |
| Methylvinylketone (MVK) | C4H6O | 70 | 2 | 55 | 0.4003 | (0.5191) | 29 | 0.8953 | (0.6389) | 23 | 2.1216 | (0.8712) | 4 |
| Butadione_23 | C4H6O2 | 86 | 2 | 86 | 0.2147 | (0.2059) | 29 | 0.6435 | (0.4616) | 23 | 1.2062 | (0.5357) | 4 |
| Acrylate_methyl (2-Propenoic Acid, methyl ester) | C4H6O2 | 86 | 2 | 85 | 0.0159 | (0.0178) | 9 | 0.0223 | (0.0149) | 16 | 0.0470 | (0.0227) | 4 |
| Acetate_vinyl (Acetic Acid, vinyl ester) | C4H6O2 | 86 | 2 | 86 | 0.0004 | (0.0012) | 9 | 0.0000 | 0.0000 | 16 | 0.0048 | (0.0095) | 4 |
| Dioxin_14_23dihydro | C4H6O2 | 86 | 2 | 58 | 0.0023 | (0.0044) | 9 | 0.0043 | (0.0059) | 16 | 0.0179 | (0.0162) | 4 |
| Cyclopentenedione | C5H4O2 | 96 | 4 | 96 | 0.0056 | (0.0080) | 9 | 0.0265 | (0.0337) | 16 | 0.0401 | (0.0326) | 4 |
| Cyclopentenone | C5H6O | 82 | 3 | 82 | 0.0825 | (0.1208) | 9 | **0.9873** | (1.1659) | 16 | 0.9221 | (0.6570) | 4 |
| Pentenone (e.g., Ethyl vinyl ketone) | C5H8O | 84 | 2 | 84 | 0.2682 | (0.4437) | 9 | 0.8946 | (0.5222) | 16 | 1.4135 | (0.6686) | 4 |
| Pentanone_cyclo | C5H8O | 84 | 2 | 84 | 0.1145 | (0.1015) | 9 | 0.3433 | (0.2471) | 16 | 0.7012 | (0.2870) | 4 |
| Butenal_2_2methyl | C5H8O | 84 | 2 | 84 | 0.0072 | (0.0064) | 9 | 0.0250 | (0.0210) | 16 | 0.0384 | (0.0136) | 4 |
| Methacrylate_methyl (Methacrylic Acid, methyl ester) | C5H8O2 | 100 | 2 | 100 | 0.0306 | (0.0333) | 9 | 0.1055 | (0.0335) | 13 | 0.1287 | (0.0537) | 4 |
| Phenol | C6H6O | 94 | 4 | 95+ | **0.4262** | (0.4242) | 25 | 0.7740 | (0.6275) | 21 | **2.4947** | (1.6182) | 4 |
| Benzene_12&13diol (sum of 2 isomers) | C6H6O2 | 110 | 4 | 109– | 0.2438 | (0.1859) | 13 | **3.1107** | (3.3461) | 17 | **3.9631** | (1.9126) | 2 |
| Benzaldehyde | C7H6O | 106 | 5 | 77 | 0.2212 | (0.1661) | 29 | 0.4717 | (0.3259) | 23 | 0.6995 | (0.2661) | 4 |
| Phenol_methyl (sum of cresol isomers') | C7H8O | 108 | 4 | 109+ | **0.4807** | (0.4799) | 25 | 0.7770 | (0.6290) | 21 | 2.0703 | (1.4093) | 4 |
| **Furans (heterocyclic OVOCs, $D = 1$)** | | | | | | | | | | | | | |
| Furan | C4H4O | 68 | 3 | 68 | **0.2680** | (0.2474) | 29 | **0.7302** | (0.4732) | 23 | **1.1090** | (0.4337) | 4 |
| Furan_25dihydro | C4H6O | 70 | 2 | 70 | 0.0083 | (0.0126) | 9 | 0.0154 | (0.0438) | 16 | 0.0071 | (0.0141) | 4 |
| Furan_tetrahydro | C4H8O | 72 | 1 | 72 | 0.0022 | (0.0027) | 9 | 0.0014 | (0.0027) | 16 | 0.0101 | (0.0067) | 4 |
| Furaldehyde_2 (Furfural) | C5H4O2 | 96 | 4 | 95 | **0.3567** | (0.2119) | 9 | **1.5298** | (1.0837) | 16 | **1.2999** | (0.6550) | 4 |
| Furaldehyde_3 | C5H4O2 | 96 | 4 | 95 | 0.0152 | (0.0135) | 9 | 0.0585 | (0.0403) | 16 | 0.0687 | (0.0330) | 4 |
| Furan_2methyl | C5H6O | 82 | 3 | 82 | **0.2847** | (0.3634) | 9 | **0.6908** | (0.4118) | 16 | **1.2105** | (0.4806) | 4 |
| Furan_3methyl | C5H6O | 82 | 3 | 82 | 0.0272 | (0.0311) | 29 | 0.0776 | (0.0582) | 23 | 0.1758 | (0.0661) | 4 |
| Furan_25dimethyl | C6H8O | 96 | 3 | 96 | 0.0328 | (0.0472) | 9 | 0.0857 | (0.0587) | 16 | 0.1808 | (0.1005) | 4 |
| Furan_2ethyl | C6H8O | 96 | 3 | 81 | 0.0167 | (0.0218) | 29 | 0.0387 | (0.0285) | 23 | 0.0821 | (0.0288) | 4 |
| Benzofuran | C8H6O | 118 | 6 | 118 | 0.0902 | (0.0666) | 9 | 0.1366 | (0.0734) | 16 | 0.2504 | (0.0957) | 4 |
| Benzofuran_methyl (sum of 4 isomers) | C9H8O | 132 | 6 | 131 | 0.0599 | (0.0444) | 9 | 0.1078 | (0.0938) | 16 | 0.1980 | (0.0363) | 4 |

Title Page

Abstract | Introduction

Conclusions | References

Tables | Figures

◀◀ | ▶▶

◀ | ▶

Back | Close

Full Screen / Esc

Printer-friendly Version

Interactive Discussion

**Table 2.** Continued.

| Name | Formula | MW | D | m/z | SW Avg | (±SD) | npnts | SE Avg | (±SD) | npnts | N Avg | (±SD) | npnts |
|---|---|---|---|---|---|---|---|---|---|---|---|---|---|
| **Methane and Inorganic Gases** | | | | | | | | | | | | | |
| Methane | CH4 | 16 | - | IR | **40.911** | (24.945) | 29 | **62.302** | (32.218) | 23 | **96.707** | (28.737) | 4 |
| Carbon Monoxide | CO | 28 | - | IR | **1000** | (0) | 29 | **1000** | (0) | 23 | **1000** | (0) | 4 |
| Carbon Dioxide | CO2 | 44 | - | IR | **18202** | (20970) | 29 | **31170** | (71256) | 23 | **17999** | (14000) | 4 |
| Tricarbon Dioxide (Carbon suboxide) | C3O2 | 68 | - | 68 | 0.0024 | (0.0030) | 9 | 0.0040 | (0.0055) | 16 | 0.0044 | (0.0042) | 4 |
| Ammonia | NH3 | 17 | - | IR | 12.530 | (8.838) | 29 | 14.797 | (6.131) | 23 | 20.761 | (16.928) | 4 |
| Nitrogen Oxide | NO | 30 | - | IR | **38.788** | (51.194) | 29 | **39.695** | (91.842) | 23 | **26.530** | (24.243) | 4 |
| Nitrogen Dioxide | NO2 | 46 | - | IR | 7.051 | (8.565) | 29 | 12.254 | (21.246) | 23 | 10.583 | (10.218) | 4 |
| Nitrous Acid | HONO | 47 | - | 46– | 2.504 | (2.827) | 16 | 4.563 | (6.049) | 17 | 4.946 | (5.254) | 2 |
| Sulfur Dioxide | SO2 | 64 | - | IR | 5.600 | (9.993) | 29 | 7.901 | (14.488) | 23 | 8.408 | (5.347) | 4 |
| Hydrochloric Acid | HCl | 36 | - | IR | 0.992 | (2.574) | 29 | 1.398 | (4.825) | 23 | 0.472 | (0.719) | 4 |
| | | | | | | | | | | | | | |
| Total ERs (mmol $(\mathrm{mol\,CO})^{-1}$) | | | | | 19356 | | | 32403 | | | 19317 | | |
| ∑ ERs for all nitrogen-containing species (mmol $(\mathrm{mol\,CO})^{-1}$) | | | | | 65 | *0.34%* | *N* | 77 | *0.24%* | *N* | 71 | *0.37%* | *N* |
| ∑ ERs for all VOCs and *% of total emissions* | | | | | 46 | *0.24%* | *VOC* | 90 | *0.28%* | *VOC* | 150 | *0.78%* | *VOC* |
| ∑ ERs for unsaturated VOCs and *% of total VOC* | | | | | 39 | *84%* | *Unsat* | 74 | *82%* | *Unsat* | 126 | *84%* | *Unsat* |
| ∑ ERs for oxygenated VOCs and *% of total VOC* | | | | | 24 | *53%* | *Oxy* | 57 | *63%* | *Oxy* | 81 | *54%* | *Oxy* |

MW = molecular weight (g mol$^{-1}$); $D$ = Degrees of unsaturation; $m/z$ = mass fragment used to quantify a species where (+) denotes measurements by the PTR-MS or PIT-MS, (−) denotes measurements by the NI-PT-CIMS, and (IR) denotes measurements by the OP-FTIR. All other measurements are by GC-MS; avg = mean; SD = standard deviation; and npts = number of points used to calculate average and standard deviation.
**Bold ER** = largest 3 ERs for each compound class.
***Bold and italic ER*** = largest 3 ERs for all VOCs.
Description of naming scheme: propane_22dimethyl is equivalent to 2,2-dimethylpropane. If the exact compound identity could not be determined, then the species are identified using general names that reflect the chemical family and formula are used. For example, hexenes (sum of 3 isomers) may include species such as cis- and trans-3-hexene. Alternative names, such as p-Cymene for 1-methyl-4-isopropylbenzene, or common abbreviations such as MEK for Butanone_2 are also included.

Title Page

Abstract | Introduction

Conclusions | References

Tables | Figures

|◄ | ►|

◄ | ►

Back | Close

Full Screen / Esc

Printer-friendly Version

Interactive Discussion

**Table 3.** Slopes and correlation coefficients ($r$) for VOC to carbon monoxide (CO) and VOC to acetonitrile ($CH_3CN$) ratios observed in biomass burning (BB) plumes from the Fourmile Canyon Fire as identified in Fig. 6.

| VOC Name | VOC vs. CO | | VOC vs. $CH_3CN$ | | Emission Sources | | | Rxn Rate Coefficient | |
| --- | --- | --- | --- | --- | --- | --- | --- | --- | --- |
| | Slope | $r$ | Slope | $r$ | BB | Urban | Biogenic | $k$OH[a] | vs. $CH_3CN$[b] |
| **Furan_2methyl** | 0.0003 | 0.88 | 0.0470 | 0.95 | yes | | | 111 | 5550 |
| Carene_3 | 0.0004 | 0.96 | 0.0654 | 0.98 | yes | | yes | 85 | 4250 |
| **Furan** | 0.0004 | 0.70 | 0.1153 | 0.95 | yes | | | 67 | 3355 |
| Butadiene_13 | 0.0002 | 0.98 | 0.0296 | 0.94 | yes | yes | | 67 | 3330 |
| Styrene | 0.0001 | 0.97 | 0.0209 | 0.94 | yes | yes | yes | 58 | 2900 |
| Propene_2methyl | 0.0004 | 0.98 | 0.0648 | 0.98 | yes | yes | | 51 | 2570 |
| **Furaldehyde_2** | 0.0003 | 0.93 | 0.0491 | 0.98 | yes | | | 48 | 2400 |
| **Benzofuran** | 0.0001 | 0.97 | 0.0210 | 0.99 | yes | | | 37 | 1860 |
| Butene_1 | 0.0004 | 0.98 | 0.0571 | 0.99 | yes | yes | | 31 | 1570 |
| Propene | 0.0040 | 0.97 | 0.6385 | 0.99 | yes | yes | | 26 | 1315 |
| Propanal | 0.0010 | 0.95 | 0.1481 | 0.90 | yes | yes | | 20 | 1000 |
| Propenal_2 | 0.0009 | 0.98 | 0.1366 | 0.98 | yes | yes | | 19 | 955 |
| p-Cymene[c] | 0.0003 | 0.97 | 0.0415 | 0.97 | yes | | yes | 15 | 750 |
| Benzaldehyde | 0.0010 | 0.98 | 0.1444 | 0.95 | yes | | yes | 14 | 700 |
| Ethene | 0.0082 | 0.97 | 1.3526 | 0.92 | yes | yes | | 8.5 | 425 |
| Benzene | 0.0019 | 0.99 | 0.2835 | 0.96 | yes | yes | | 1.2 | 60 |
| Butanone_2 (MEK) | 0.0010 | 0.93 | 0.1640 | 0.94 | yes | yes | yes | 1.2 | 60 |
| **Benzonitrile** | 0.0003 | 0.88 | 0.0499 | 0.94 | yes | | | 1.0 | 50 |
| Butadione_23 | 0.0002 | 0.77 | 0.0384 | 0.89 | yes | | yes | 0.25 | 12.5 |
| **Acetonitrile** | 0.0062 | 0.96 | 1.0000 | 1.00 | yes | | | 0.020 | 1 |

**Bold** face denotes VOCs that are the best available BB markers.
[a] Rxn Rate Coefficient $\times 10^{12}$ = first order reaction rate coefficient of VOC + OH reaction at STP.
[b] Ratio of rxn rate coefficients for VOC vs. acetonitrile ($CH_3CN$) $\times 10^{12}$ at STP.
[c] Benzene_1methyl_4isopropyl.
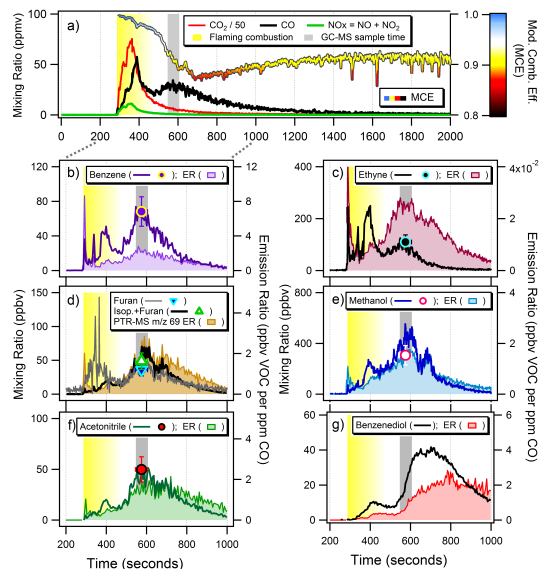
**Figure 1.** Temporal profiles of mixing ratios and emission ratios (ER) of select gases and the modified combustion efficiency (MCE) for an example laboratory burn of Emory Oak Woodland fuel from Fort Huachuca, Arizona. **(a)** Mixing ratios of $CO_2$, CO, and NOx measured by OP-FTIR. The MCE trace is colored by the key and scale on the right. The vertical bars represent the flaming combustion phase of the laboratory burn (yellow) and the GC-MS sample acquisition time (grey). **(b–f)** Discrete GC-MS measured mixing ratios are shown as markers. **(b–g)** Mixing ratios measured by PTR-MS (benzene, $m/z$ 69 = isoprene + furan + other, and acetonitrile), OP-FTIR (furan, ethyne, and methanol), and NI-PT-CIMS (benzenediol) are shown as lines and the corresponding VOC to CO ERs are shown as filled traces.

Full Screen / Esc

Printer-friendly Version

Interactive Discussion
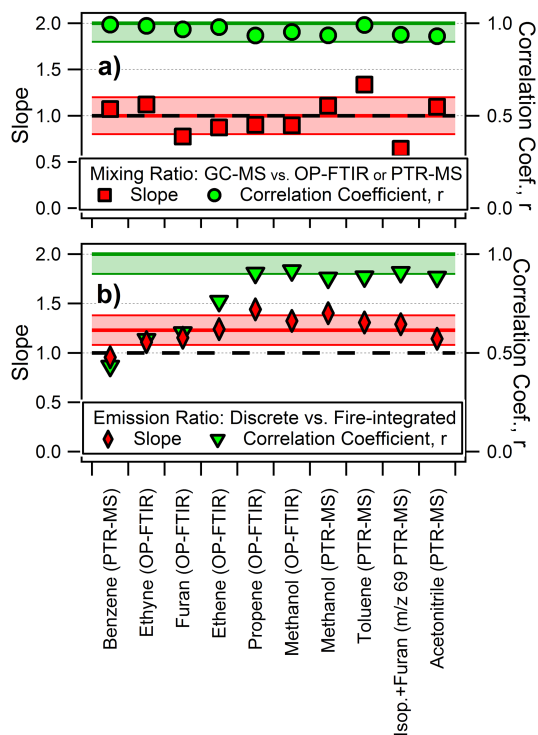


**Figure 2.** Slopes and correlation coefficients, $r$, determined from correlation plots of **(a)** mixing ratios measured by the GC-MS vs. the average mixing ratio measured by the OP-FTIR or PTR-MS during the GC-MS sample acquisition time and **(b)** discrete vs. fire-integrated emission ratios of select VOCs relative to CO as measured by the OP-FTIR or PTR-MS. The black dashed line represents slopes equal to 1. The average of the slopes and the standard deviation is shown by the red shaded bands. The green bands represent $r > 0.90$.
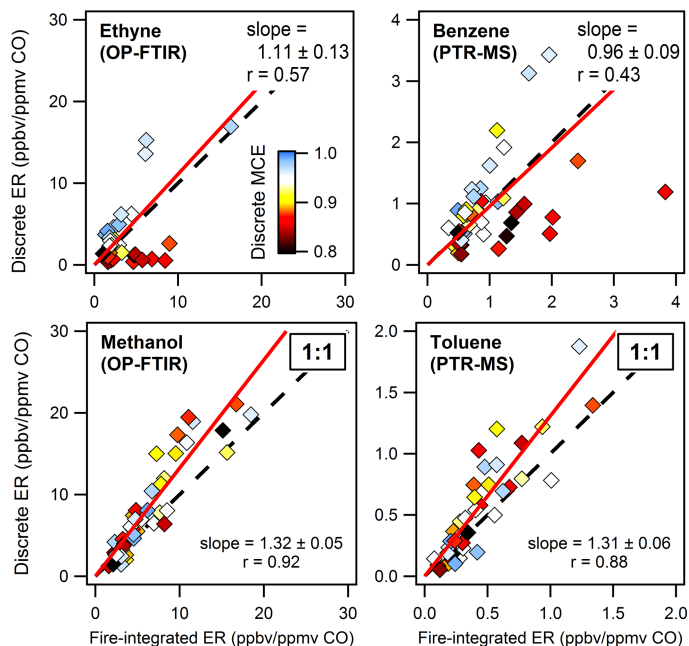
**Figure 3.** Correlation plots of the discrete vs. fire-integrated emission ratios (ER) for ethyne and methanol measured by the OP-FTIR and benzene and toluene measured by the PTR-MS. Each data point represents one biomass burn and are colored by the modified combustion efficiency (MCE) corresponding to the discrete sampling times of the GC-MS. MCE values near unity are associated with flaming combustion and lower MCE values are associated with smoldering combustion. The linear 2-sided regression lines forced through the origin are shown as red lines and the 1 : 1 ratio is shown by the dashed lines.
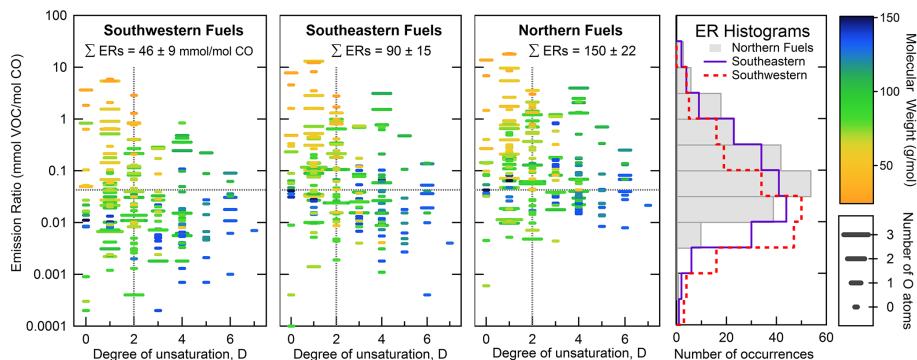
**Figure 4.** Discrete molar emission ratios for all VOCs reported in Table 2 as a function of the degree of unsaturation, $D$, for each fuel region. Emission ratios are colored by the corresponding molecular weight and the marker width represents the corresponding number of oxygen (O) atoms. The dashed lines represent the median values for all VOCs from all fuel regions (ER = 0.0427 mmol mol$^{-1}$ CO and $D$ = 2). The histogram on the right summarizes the distribution of molar emission ratios for each fuel region.

Title Page

Abstract | Introduction

Conclusions | References

Tables | Figures

|◄ | ►|

◄ | ►

Back | Close

Full Screen / Esc

Printer-friendly Version

Interactive Discussion
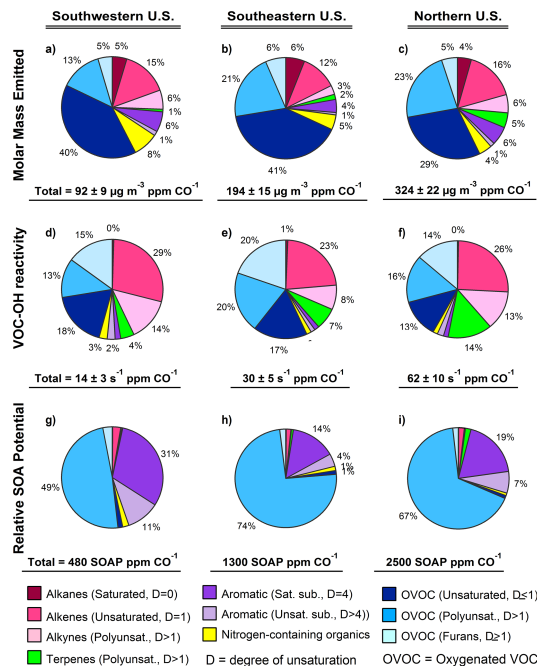
**Figure 5.** Contributions of (non-methane) VOCs reported in Table 2 to **(a–c)** the molar mass emitted, **(d–f)** OH reactivity, and **(g–i)** relative SOA potential for the southwestern, southeastern, and northern fuel regions. Totals for each fuel region are shown below each pie chart.
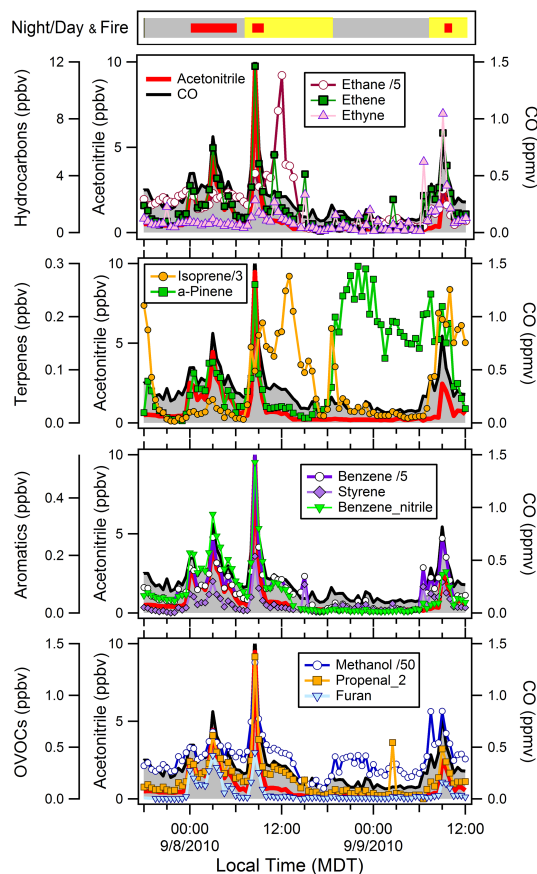
**Figure 6.** Time series of ambient air measurements in Boulder, Colorado, during the Fourmile Canyon Fire. The top bar indicates nighttime (grey), daytime (yellow), and biomass burning plumes (red markers). CO and acetonitrile are included in all 4 panels.
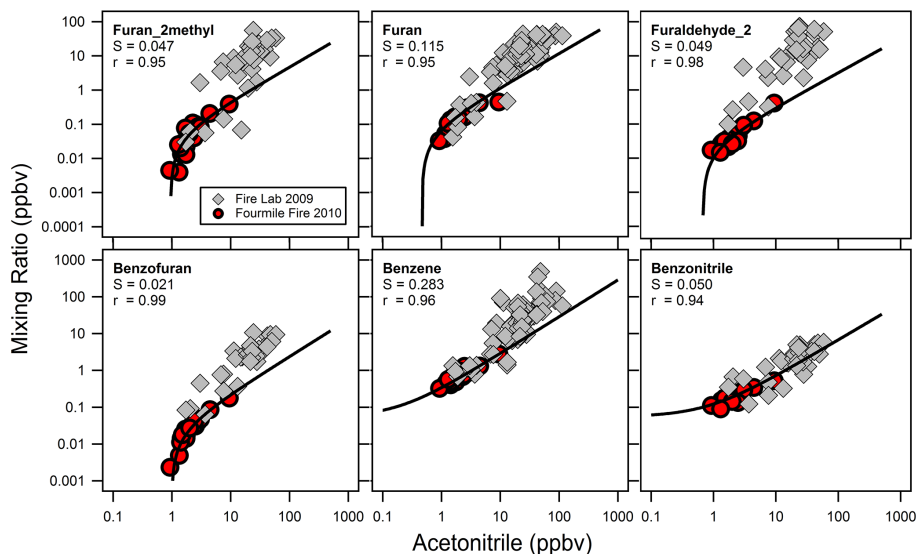
**Figure 7.** Correlation plots of VOCs vs. acetonitrile for all 56 laboratory biomass burns (grey markers) and Fourmile Canyon Fire (red markers correspond to the BB plume identified in Fig. 6).